


ORIGINAL RESEARCH

# SENP1 Protects Against Pressure Overload-Induced Cardiac Remodeling and Dysfunction Via Inhibiting STAT3 Signaling

Dan Yang, MD; Di Fan, MD; Zhen Guo, MD; Fang-Yuan Liu, MD; Ming-Yu Wang, MD; Peng An, MD; Zheng Yang, MD; Qi-Zhu Tang , MD, PhD

**BACKGROUND:** SENP1 (sentrin/small ubiquitin-like modifier-specific protease 1) has emerged as a significant modulator involved in the pathogenesis of a variety of human diseases, especially cancer. However, the regulatory roles of SENP1 in cardiovascular biology and diseases remain controversial. Our current study aims to clarify the function and regulation of SENP1 in pressure overload-induced cardiac remodeling and dysfunction.

**METHODS AND RESULTS:** We used a preclinical mouse model of transverse aortic constriction coupled with in vitro studies in neonatal rat cardiomyocytes to study the role of SENP1 in cardiac hypertrophy. Gene delivery system was used to knock-down or overexpress SENP1 in vivo. Here, we observed that SENP1 expression was significantly augmented in murine hearts following transverse aortic constriction as well as neonatal rat cardiomyocytes treated with phenylephrine or angiotensin II. Cardiac-specific SENP1 knockdown markedly exacerbated transverse aortic constriction-induced cardiac hypertrophy, systolic dysfunction, fibrotic response, and cellular apoptosis. In contrast, adenovirus-mediated SENP1 overexpression in murine myocardium significantly attenuated cardiac remodeling and dysfunction following chronic pressure overload. Mechanistically, JAK2 (Janus kinase 2) and STAT3 (signal transducer and activator of transcription 3) acted as new interacting partners of SENP1 in this process. SENP1-JAK2/STAT3 interaction suppressed STAT3 nuclear translocation and activation, ultimately inhibiting the transcription of prohypertrophic genes and the initiation of hypertrophic response. Furthermore, cardiomyocyte-specific STAT3 knockout mice were generated to validate the underlying mechanisms, and the results showed that STAT3 ablation blunted the cardiac hypertrophy-promoting effects of SENP1 deficiency. Additionally, pharmacological inhibition of SENP1 by Momordin Ic amplified cardiac remodeling post-transverse aortic constriction.

**CONCLUSIONS:** Our study provided evidence that SENP1 protected against pressure overload-induced cardiac remodeling and dysfunction via inhibiting STAT3 signaling. SENP1 supplementation might constitute a new promising treatment against cardiac hypertrophy. Notably, cardiovascular side effects should be seriously considered while applying systemic SENP1 blockers to suppress tumors.

**Key Words:** cardiac remodeling ■ JAK2 ■ pressure overload ■ SENP1 ■ STAT3

**C**ardiac hypertrophy, a complex cardiovascular sequela, is caused by a spectrum of hypertensive cardiac stress such as myocardial injury, chronic mechanical overload, neurohormonal stimuli, and genetic mutations.<sup>1</sup> Characterized with cardiomyocyte enlargement, structural abnormalities, and cardiac

dysfunction, cardiac hypertrophy represents a critical predisposing factor for cardiovascular events. Without appropriate intervention, cardiac hypertrophy may ultimately progress into end-stage heart failure, a growing public health problem worldwide with high morbidity and mortality.<sup>2</sup> Cardiac hypertrophy acts as a significant

Correspondence to: Qi-Zhu Tang, MD, PhD, Department of Cardiology, Renmin Hospital of Wuhan University, Hubei Key Laboratory of Metabolic and Chronic Diseases, Wuhan University at Jiefang Rd 238, Wuhan 430060, PR China. Email: [qztang@whu.edu.cn](mailto:qztang@whu.edu.cn)

Supplemental Material is available at <https://www.ahajournals.org/doi/suppl/10.1161/JAHA.122.027004>

For Sources of Funding and Disclosures, see page 17.

© 2022 The Authors. Published on behalf of the American Heart Association, Inc., by Wiley. This is an open access article under the terms of the [Creative Commons Attribution-NonCommercial](https://creativecommons.org/licenses/by-nc/4.0/) License, which permits use, distribution and reproduction in any medium, provided the original work is properly cited and is not used for commercial purposes.

JAHA is available at: [www.ahajournals.org/journal/jaha](http://www.ahajournals.org/journal/jaha)

## CLINICAL PERSPECTIVE

### What Is New?

- Our study provides evidence that SENP1 (sentrin/small ubiquitin-like modifier -specific protease 1) protects against cardiac remodeling and dysfunction triggered by long-term pressure overload.
- SENP1 could directly interact with JAK2 and STAT3 in cardiomyocytes, resulting in the inhibition of STAT3 activation and STAT3 nuclear translocation, thus bringing benefits to cardiac injury caused by chronic pressure overload.

### What Are the Clinical Implications?

- Approaches to stimulate or stabilize SENP1 expression might be achieved to mitigate cardiac hypertrophy.
- Considering the detrimental effects of SENP1 deficiency in heart diseases, cardiovascular side effects should be seriously considered while applying systemic SENP1 blockers to suppress tumors.

## Nonstandard Abbreviations and Acronyms

<b>ANP</b>	atrial natriuretic peptide
<b>I/R</b>	ischemia/reperfusion
<b>NRCMs</b>	neonatal rat cardiomyocytes
<b>SENPs</b>	Sentrin/small ubiquitin-like modifier-specific proteases
<b>TAC</b>	transverse aortic constriction

target of therapeutic strategies for patients suffering from heart failure. In the past decades, despite multiple cellular and molecular signaling pathways that have been identified in the initiation and progression of cardiac hypertrophy, the pathogenesis of cardiac hypertrophy remains incompletely understood.<sup>3-5</sup> Thus, identifying novel molecular targets and signaling networks involved in cardiac hypertrophy continues to be of great value and interest.

SUMOylation is an ubiquitin-like post-translational modification that is involved in the dynamic regulation of a range of cellular processes, including immune responses, tumorigenesis, apoptosis, DNA damage repair, etc.<sup>6</sup> Generally, the conjugation of SUMO (small ubiquitin-like modifier) proteins are mediated by a cascade of enzymes comprised of E1-activating enzyme, E2 conjugase, and E3 ligases, while the deSUMOylation process is precisely regulated by SENPs (sentrin/

SUMO-specific proteases), which have the capability of removing the SUMO proteins from the modified proteins. The SENP family consists of 6 members, including SENP1, SENP2, SENP3, SENP5, SENP6, and SENP7, with differences in their tissue distribution, cellular localization, and catalytic properties.<sup>7,8</sup> Among all the identified SENPs, SENP1 is the first discovered as well as the most widely studied. An increasing number of research suggests that SENP1 may serve as an effective prognostic biomarker and a suitable therapy strategy for solid tumors and hematologic malignancies, and notably, some Food and Drug Administration-approved drugs are shown to target SENP1 and treat cancer, indicating the clinical value of SENP1 inhibitors.<sup>9</sup>

In recent years, emerging studies have provided evidence that SENP1 is expressed in the heart tissue and may exert profound roles in the initiation and progression of cardiovascular disorders. SENP1 was initially shown to protect against myocardial ischemia/reperfusion (I/R) injury. In vivo and in vitro experimental data have indicated that SENP1 deficiency worsened cardiac function and accelerated cardiomyocyte apoptosis, and the cardioprotective roles of SENP1 in I/R is HIF1 $\alpha$ -dependent.<sup>10</sup> Another study demonstrated that cardiomyocyte-specific overexpression of SENP1 was associated with mitochondrial abnormalities and dysfunction through calcineurin-NFAT/MEF2C-PGC-1 $\alpha$  signaling.<sup>11</sup> These results suggest that SENP1 may serve as a significant candidate for cardiovascular diseases. However, up to date, studies focusing on the regulatory role of SENP1 in cardiac hypertrophy caused by chronic pressure overload are limited.

In this study, we explored the contribution of SENP1 in chronic pressure overload via transverse aortic constriction (TAC), a well-established mouse cardiac hypertrophy model. We demonstrated that hypertrophic stimuli led to abnormal induction of SENP1 both at mRNA and protein levels in cardiomyocytes. Our results also elucidated that pressure overload-induced cardiac hypertrophy and dysfunction were deteriorated in the absence of SENP1 but improved with exogenous SENP1 supplementation, indicating the cardioprotective roles of SENP1 against cardiac hypertrophy. Further molecular study unraveled that STAT3 may act as a new interacting partner of SENP1 in this process.

## METHODS

The data supporting the findings of this study are available from the corresponding author upon reasonable request.

## Animals

All animal care and procedures were performed in compliance with the guidelines of the National Institutes of Health (revised 2011) and authorized by the Animal Care and Use Committee of Renmin Hospital of Wuhan University (approve number: WDRM20191209). In animal experiments, genetic background, age- and sex-matched mice were randomly divided into indicated groups. Experiments and subsequent data analysis were performed blindly. Male C57BL/6 mice (8–10 weeks old, 23.5–27.5 g) were acquired from the Institute of Laboratory Animal Science, Chinese Academy of Medical Sciences (Beijing, China). STAT3<sup>flox/flox</sup> mice, maintained on a C57BL/6 genetic background, were obtained from Cyagen (Suzhou, China). Mice carrying the  $\alpha$ -myosin heavy chain ( $\alpha$ -MHC)-MerCreMer (MCM) transgene were acquired from the Jackson Laboratory. All mice were fed in a specific pathogen-free environment (temperature: 20–25 °C; humidity: 50±5%; with 12 hours light/dark cycles) with ad libitum access to sterile water and food. Before animal experimental procedures, all the animals were adaptively fed for 1 week. Gene transfer-based approaches were used to downregulate or upregulate SENP1 levels.<sup>12,13</sup> To specifically downregulate SENP1 in murine hearts, the mice received a single intravenous injection of adeno-associated virus serotype 9 (AAV9) ( $1 \times 10^{11}$  viral genome per mouse) carrying sh*Senp1*, which was constructed by Designgene Biotechnology (Shanghai, China), and AAV9 containing nonspecific short hairpin RNA (shRNA) was used as control. To overexpress SENP1 in mouse hearts, we performed a single intramyocardial injection of  $1 \times 10^9$  adenoviral (Ad) genome particles (Designgene Biotechnology, Shanghai, China) carrying *Senp1*, and AdGFP (green fluorescence protein) was used as controls. Four weeks after AAV9 injection or 1 week after adenoviral injection, mice were randomly subjected to TAC operation to induce pressure overload-cardiac hypertrophy model or a sham operation as a control. The cardiac function of these mice was measured 4 weeks post-surgery, and then mice were euthanized with excess pentobarbital sodium (200 mg/kg; intraperitoneally). The ratios of heart weight to tibia length were calculated. The mouse hearts were frozen in liquid nitrogen and then stored at –80 °C for subsequent molecular experiments, or arrested in remission in 10% potassium chloride and fixed in 10% formalin for histological analysis. To further verify the hypothesis that the modulatory role of SENP1 in pressure overload-induced cardiac hypertrophy was STAT3-dependent, a mouse model of STAT3 conditional knockout was generated by crossing STAT3<sup>flox/flox</sup> mice with mice carrying  $\alpha$ -MHC-MCM transgene. For cardiac specific-knockout of STAT3, pharmaceutical-grade tamoxifen dissolved

in corn oil was injected into 6-week-old mice for 5 consecutive days (25 mg/kg per day, intraperitoneally).<sup>12</sup> The controls were also injected with equal dose of tamoxifen. For the treatment of Momordin Ic (Mc), mice were intraperitoneally injected with Mc at 10 mg/kg daily for 20 consecutive days, and dimethyl sulphoxide was used as vehicle control.<sup>14</sup>

## Transverse Aortic Constriction

Murine cardiac hypertrophy was induced by TAC as previously described.<sup>15,16</sup> In brief, mice were anesthetized by intraperitoneal injection of sodium pentobarbital (50 mg/kg). In the absence of pain stimulation reflex, mice were fixed on the thermostatic heating pad to open the left chest at the second intercostal space, and then the thoracic aorta was exposed by blunt dissection. Next, a 7–0 silk suture was used to band the aortic arch against a 27-gauge needle between the innominate and left common carotid artery. Subsequently, the 27-G needle was quickly removed, leaving a discrete region of constriction. Sham-operated mice were subjected to the same surgical procedure except for constricting the aorta. Adequate constriction of the aorta was examined by Doppler analysis and the mice with unsuccessful surgery were removed from experimental groups. All surgical procedures were performed blindly.

## Echocardiography

Echocardiography was performed as we previously described.<sup>17,18</sup> After anesthetization with isoflurane (1.5%–2%), mice received transthoracic echocardiography for the evaluation of cardiac function. M-mode tracings were used to measure echocardiographic parameters including left ventricular internal dimension diastolic, left ventricular internal dimension systolic, left ventricular ejection fraction, and left ventricular fractional shortening, which were averaged from 3 to 5 consecutive cardiac cycles.

## Histological Analysis

Hearts were harvested from the euthanized mice, arrested in remission in 10% potassium chloride, and then immersion fixed in 10% formalin. After being embedded in paraffin, the heart tissues were transversely cut into 5- $\mu$ m-thick sections. To analyze the cardiomyocyte cross-sectional area, the tissue section was stained with hematoxylin and eosin and examined under bright field microscopy (Aperio VERSA 8, Leica). To evaluate collagen deposition, cardiac sections were stained with Picrosirius red. The images were analyzed by Image-Pro Plus software (version 6.0). More than 100 myocytes in the examined sections were outlined in each group of mice.

## Cell Culture and Treatments

Neonatal rat cardiomyocytes (NRCM) were prepared as previously described.<sup>16</sup> Briefly, hearts were removed from neonatal Sprague–Dawley rats (1 to 2 days old) and digested with 0.125% trypsin. Then, the harvested cells were centrifuged, resuspended, and cultured in DMEM/F12 (Gibco) with 15% fetal bovine serum (Gibco) for 90 minutes, and NRCMs, which were in the suspended medium, were plated at a density of  $1 \times 10^6$  cells/mL. The isolated NRCMs were then cultured in the medium consisting of 15% fetal bovine serum, BrdU (0.1 mmol/L, to prevent fibroblast proliferation), and penicillin/streptomycin. After 48 hours, the NRCMs were starved in serum-free DMEM/F12 medium for 12 hours, subsequently, NRCMs were treated with phenylephrine (50  $\mu$ mol/L) or angiotensin II (1  $\mu$ mol/L) to induce hypertrophy. To knockdown SENP1 expression, adenoviruses carrying rat *shSenp1* were used, and shRNA was the nontargeting control. For the overexpression of SENP1, cultured cells were infected with Ad*Senp1*. Cells were infected with adenoviruses at a multiplicity of infection of 100 for 24 hours. For further investigations of the molecular mechanisms involved, STAT3 was silenced by siRNA transfection; meanwhile, some STAT3-associated signaling inhibitors dissolved in dimethyl sulphoxide were also used for the investigation of molecular mechanisms: Smyd2 inhibitor LLY-507 (5  $\mu$ mol/L for 24 hours), HDAC6 inhibitor ACY-1215 (0.5  $\mu$ mol/L for 24 hours), ErbB2 inhibitor AG825 (10  $\mu$ mol/L for 24 hours), and JAK2 inhibitor AG490 (10  $\mu$ mol/L for 6 hours).<sup>19–22</sup> H9c2 cells, purchased from the Cell Bank of the Chinese Academy of Sciences (Shanghai, China), were also used in this study. H9c2 cells were cultured in DMEM (Gibco) supplemented with 10% fetal bovine serum.

## Western Blots

Proteins were prepared from frozen left ventricles or cultured cells. Whole-cell lysates and nuclear protein fractions were separated by RIPA lysis buffer (Servicebio, Wuhan, China) and a commercial kit (Thermo Fisher Scientific) following manufacturers' protocols, respectively. The extracted proteins were quantified by a BCA Protein Assay Kit (Thermo Scientific, 23227). Subsequently, 50  $\mu$ g of each protein sample was fractionated by SDS-PAGE and electro-transferred onto polyvinylidene fluoride membranes (Millipore, IPVH00010), which were then blocked with Tris-buffered saline containing 5% bovine serum albumin for 1 hour. And then the membranes were incubated with primary antibodies, including anti-GAPDH (Cell Signaling Technology, CST, 2118, 1:1000), anti-Lamin B1 (Abcam, ab16048, 1:1000), anti-SENP1 (santa cruz, sc-271360, 1:200), anti-atrial natriuretic peptide (ANP) (santa cruz, sc-20158, 1:200), anti-BNP (brain

natriuretic peptide) (Abcam, ab239510, 1:1000), anti-Jak2 (CST, 3230S, 1:1000), anti-P-Jak2 (CST, 3776, 1:1000), anti-Stat3 (CST, 9139S, 1:1000), anti-P-Stat3 (CST, 9145, 1:1000), anti-Bax (Bcl-2-associated X protein) (CST, 2772, 1:1000), anti-Bcl-2 (B-cell lymphoma-2) (Abcam, ab196495, 1:1000), anti-PTEN (phosphatase and tensin homolog) (CST, 9559, 1:1000), anti-P-AKT (phosphorylated protein kinase B) (CST, 4060, 1:1000), anti-AKT (protein kinase B) (CST, 4691, 1:1000), anti-HIF1 $\alpha$  (CST, 36169S, 1:1000), anti-Sirt1 (sirtuin 1) (CST, 8469, 1:1000), and anti-Sirt3 (sirtuin 3) (CST, 5490, 1:1000), at 4 °C overnight followed by incubation with secondary antibodies (1:10000) for 1 hour at room temperature. The signals were detected by the ECL system, visualized using ChemiDoc XRS+(Bio-Rad), and quantified using Image Lab software. The expression levels of specific proteins were normalized to GAPDH for the total lysates or to Lamin B1 for the nuclear proteins.

## RNA Isolation and Quantitative Real-Time Polymerase Chain Reaction

Total RNA of frozen heart tissues and cultured cells was extracted using TRIzol (Invitrogen, 15596–026) and converted to cDNA using Transcriptor First Strand cDNA Synthesis Kit [Roche (Basel, Switzerland), 04897030001] following manufacturers' protocols. Quantitative real-time polymerase chain reaction (qRT-PCR) was performed using Light Cycler 480 SYBR Green 1 Master Mix (Roche, 04887352001). The details about all primer sequences are listed in Table S1, and GAPDH is used as the endogenous reference gene.

## Immunoprecipitation

Immunoprecipitation was conducted according to the manufacturer's instructions for Protein A+G Agarose (Beyotime, Shanghai, China). Briefly, the freshly isolated heart tissue or cell lysates were incubated overnight with rotation at 4 °C with anti-immunoglobulin G antibody, anti-STAT3 antibody, or anti-JAK2 antibody. The lysates with primary antibody were then mixed with Protein A+G agarose beads and incubated with rotation at 4 °C for 3 hours. Beads containing immunoprecipitated proteins were then washed 5 times with ice-cold PBS and boiled with 1 $\times$ SDS loading buffer. The supernatant was then subjected to immunoblotting for the examination of the target proteins.

## Immunofluorescence Staining

Immunofluorescence staining was performed as previously described.<sup>17</sup> Briefly, immunofluorescence staining was performed on paraffin-embedded sections and fixed cells using antibodies to SENP1 (santa cruz, sc-271360, 1:25), sarcomeric alpha actinin (Abcam,

ab68167, 1:100), alpha actinin (CST, 69758S, 1:100), cardiac Troponin I (Abcam, ab155047, 1:100), P-Stat3 (CST, 9145, 1:100), Stat3 (CST, 30835S, 1:100), and Jak2 (CST, 3230S, 1:100) at 4 °C overnight. The following day, the sections and cells were incubated with Alexa Fluor 488 goat anti-rabbit or 568 goat anti-mouse secondary antibody (1:200, Invitrogen) for 60 minutes at 37 °C. Nuclei were stained by 4',6-diamidino-2-phenylindole (Invitrogen, S36939). Fluorescein isothiocyanate-conjugated wheat germ agglutinin (Invitrogen) was used for the detection of cell membranes following manufacturers' protocols. Fluorescence images were captured using OLYMPUS DX51 fluorescence microscope (Tokyo, Japan) and analyzed by Image-Pro Plus software (version 6.0).

### Immunohistochemistry

Paraffin-embedded mouse heart tissues were incubated with antibodies to SENP1 (Abcam, ab236094, 1:100), CD45 (Abcam, ab10558, 1:200), and CD68 (Abcam, ab125212, 1:100) overnight. After washing in PBS, the tissue sections were incubated with anti-rabbit/mouse EnVision™ +/horseradish peroxidase reagent at a temperature of 37 °C for 30 to 60 minutes, and then reacted with 3,3'-diaminobenzidine for the detection of the positive areas (Gene Technology, Shanghai, China; GK600705). Then the sections were counterstained with hematoxylin and mounted with coverslips. The images were taken under bright field microscopy (Nikon H550L (Tokyo, Japan)) and analyzed using Image-Pro Plus (version 6.0).

### Statistical Analysis

All data in this study were expressed as mean±SD and analyzed by GraphPad Prism 8.0 (GraphPad Prism Software Inc., San Diego, CA, USA). Data normality was determined by Kolmogorov–Smirnov test. For non-normal data, a nonparametric statistical analysis was performed using Mann–Whitney test for 2 groups and Kruskal–Wallis test for multiple groups. Unpaired Student *t*-test was used for comparison between 2 groups. One-way and 2-way ANOVA followed by Bonferroni post-test was applied when comparing at least 3 experimental groups. *P*<0.05 was considered statistically significant.

## RESULTS

### Hypertrophic Stimulation Leads to Upregulation of SENP1 In Vivo and Vitro

To determine whether the expression of SENP1 is associated with cardiac hypertrophy, we first established a murine model of cardiac hypertrophy induced by TAC. Wild-type mice were subjected to 1, 2, 3, 4,

and 8 weeks of TAC surgery, these time points were designed to capture the optimal time for SENP1 up-regulation. Histological analysis revealed that TAC-operated mice exhibited time-dependent increases in the cardiomyocyte cross-sectional areas (Figure S1A), and echocardiography showed that cardiac contractile function was preserved at weeks 1 and 2 but markedly decreased from weeks 3 post-TAC (Figure S1B). These results suggested the successful establishment of cardiac hypertrophy models. Meanwhile, it also revealed that pressure overload initially contributed to adaptive hypertrophy, while sustained pressure overload induced maladaptive hypertrophy and cardiac dysfunction. Our qRT-PCR results showed that SENP1 levels were significantly increased after TAC operation, and notably, SENP1 upregulation peaked at 4 weeks post-TAC (Figure S1C). To validate this observation, we detected SENP1 protein levels in mouse hypertrophic heart tissues as well as NRCMs treated with pro-hypertrophic stimulus based on different experimental approaches. The results from western blots suggested that SENP1 was upregulated at protein levels in mouse hypertrophic hearts induced by TAC compared with sham control hearts (Figure 1A). Consistently, immunohistochemistry results showed that SENP1 expression was elevated in response to TAC-induced cardiac hypertrophy (Figure 1B). Immunofluorescence staining of heart tissue sections with anti-SENP1 and anti-Troponin I demonstrated that SENP1 was significantly elevated in the hypertrophic myocardium compared with controls (Figure S1D). To mimic hypertrophic conditions in NRCMs, we treated the cells with phenylephrine (50 μmol/L) or angiotensin II (1 μmol/L) at different time points. Results from qRT-PCR revealed that the expression of SENP1 was increased in a time-dependent manner and remained at a high level for 24 hours by these hypertrophic stimuli when compared with the control group (Figure S1E and S1F). Consistently, results from immunoblotting and immunofluorescence staining revealed the increased expression of SENP1 proteins in hypertrophic NRCMs (Figure 1C through 1F). Collectively, these results indicated that the expression of SENP1 can be markedly upregulated by hypertrophic stress.

### Pressure Overload-Induced Cardiac Remodeling and Dysfunction Are Aggravated in the Absence of SENP1

To investigate the functional role of SENP1 in pressure overload-induced cardiac hypertrophy, we transduced murine hearts with AAV9 vectors carrying sh*Senp1*, and shRNA served as controls (Figure S2A). Figure S2B showed the inhibitory efficiency of 3 constructed AAV9 carrying sh*Senp1* on SENP1 gene, among which the second was preferred. Experimental

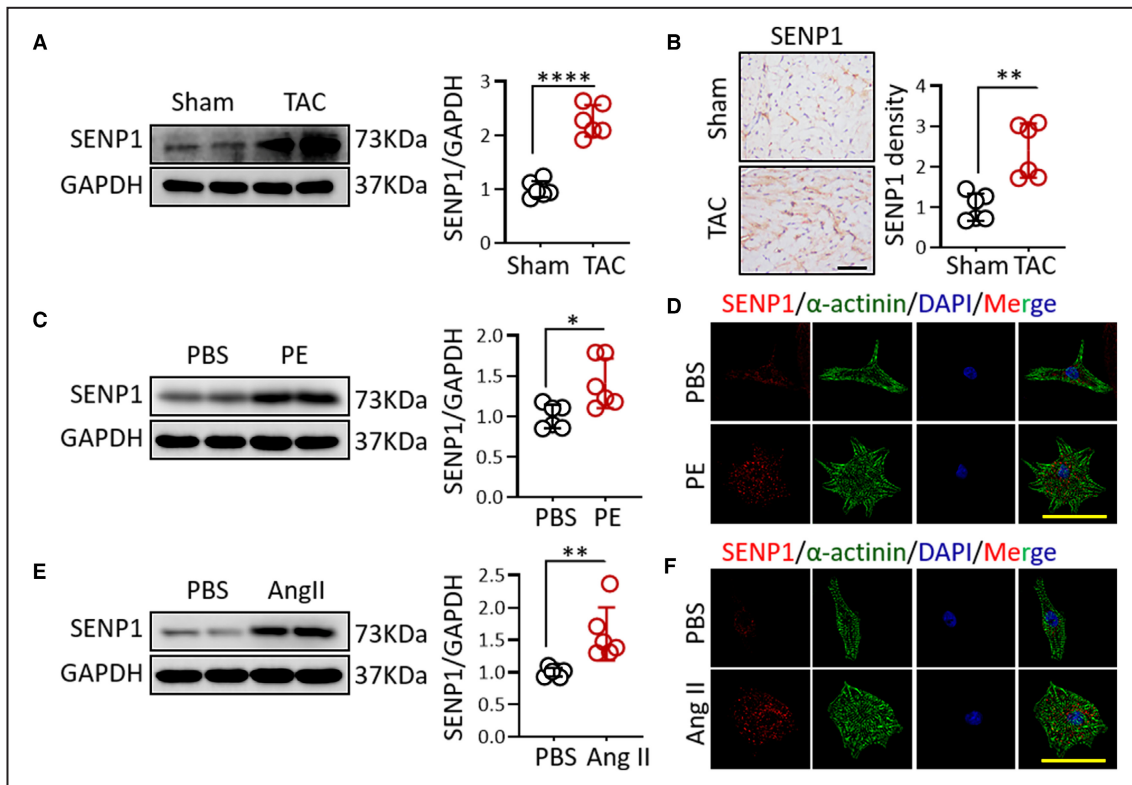


**Figure 1. Hypertrophic stimulation leads to upregulation of SENP1 (Sentrin/small ubiquitin-like modifier-specific protease 1) in vivo and in vitro.**

**A**, Representative western blot analysis and quantitative data for SENP1 expression in murine heart tissues with sham operation or 4 weeks of transverse aortic constriction (n=6 per group). Protein expression was quantified and normalized to GAPDH. **B**, Immunohistochemistry staining and quantitative data for SENP1 in the myocardium of wild-type mouse hearts with sham or transverse aortic constriction operation for 4 weeks (n=6 per group). Scale bar, 50  $\mu$ m. **C**, Representative western blot analysis and quantitative data for SENP1 protein levels in phenylephrine (50  $\mu$ mol/L) or PBS-treated neonatal rat cardiomyocytes for 24 hours (n=6 independent experiments). Protein expression was quantified and normalized to GAPDH. **D**, Representative images for immunofluorescence staining of  $\alpha$ -actinin (green) and SENP1 (red) in neonatal rat cardiomyocytes stimulated with phenylephrine (50  $\mu$ mol/L) or vehicle for 24 hours. Scale bar, 50  $\mu$ m. **E**, Representative western blot analysis and quantitative data for SENP1 protein levels in angiotensin II (1  $\mu$ mol/L) or PBS treated neonatal rat cardiomyocytes for 24 hours (n=6 independent experiments). Protein expression was quantified and normalized to GAPDH. **F**, Representative images for immunofluorescence staining of  $\alpha$ -actinin (green) and SENP1 (red) in neonatal rat cardiomyocytes stimulated with angiotensin II (1  $\mu$ mol/L) or vehicle for 24 hours. Scale bar, 50  $\mu$ m. Values represent the mean $\pm$ SD. All data were analyzed by unpaired Student *t*-test. \**P*<0.05; \*\**P*<0.01; \*\*\**P*<0.001; \*\*\*\**P*<0.0001. Ang II indicates angiotensin II; DAPI, 4',6-diamidino-2-phenylindole; NRCMs, neonatal rat cardiomyocytes; SENP1, sentrin/small ubiquitin-like modifier-specific protease 1; and TAC, transverse aortic constriction.

data from immunoblotting also exhibited that the levels of SENP1 in the myocardium were markedly decreased after sh*Senp1* treatment compared with the shRNA-transduced group (Figure 2A). Four weeks after intravenous injection, mice were randomly allocated to TAC surgery or sham operations. The impact of SENP1 deficiency on cardiac hypertrophy was then assessed. The cardiomyocyte cross-sectional areas and hypertrophic marker levels in AAV9-shRNA and AAV9-sh*Senp1* treated mice were similar under unstimulated basal conditions. Notably, after 4 weeks of TAC induction, mice deficient in SENP1 exhibited enlarged hearts and elevated heart weight to tibia length

ratios (Figure 2B and 2C). Echocardiography was also performed to assess the functional changes of mice in each group. As shown in Figure 2D and 2E, mice that received AAV9-sh*Senp1* exhibited significantly increased left ventricular internal dimension systolic and left ventricular internal dimension diastolic but decreased left ventricular ejection fraction and left ventricular fractional shortening compared with the AAV9-shRNA controls after TAC (Figure 2D and 2E). Hematoxylin and eosin staining showed the exaggerated effects of SENP1 deficiency on TAC-induced cardiac hypertrophy (Figure 2F). Accordingly, SENP1 loss led to the upregulation of ANP and BNP (Figure 2G). Moreover,

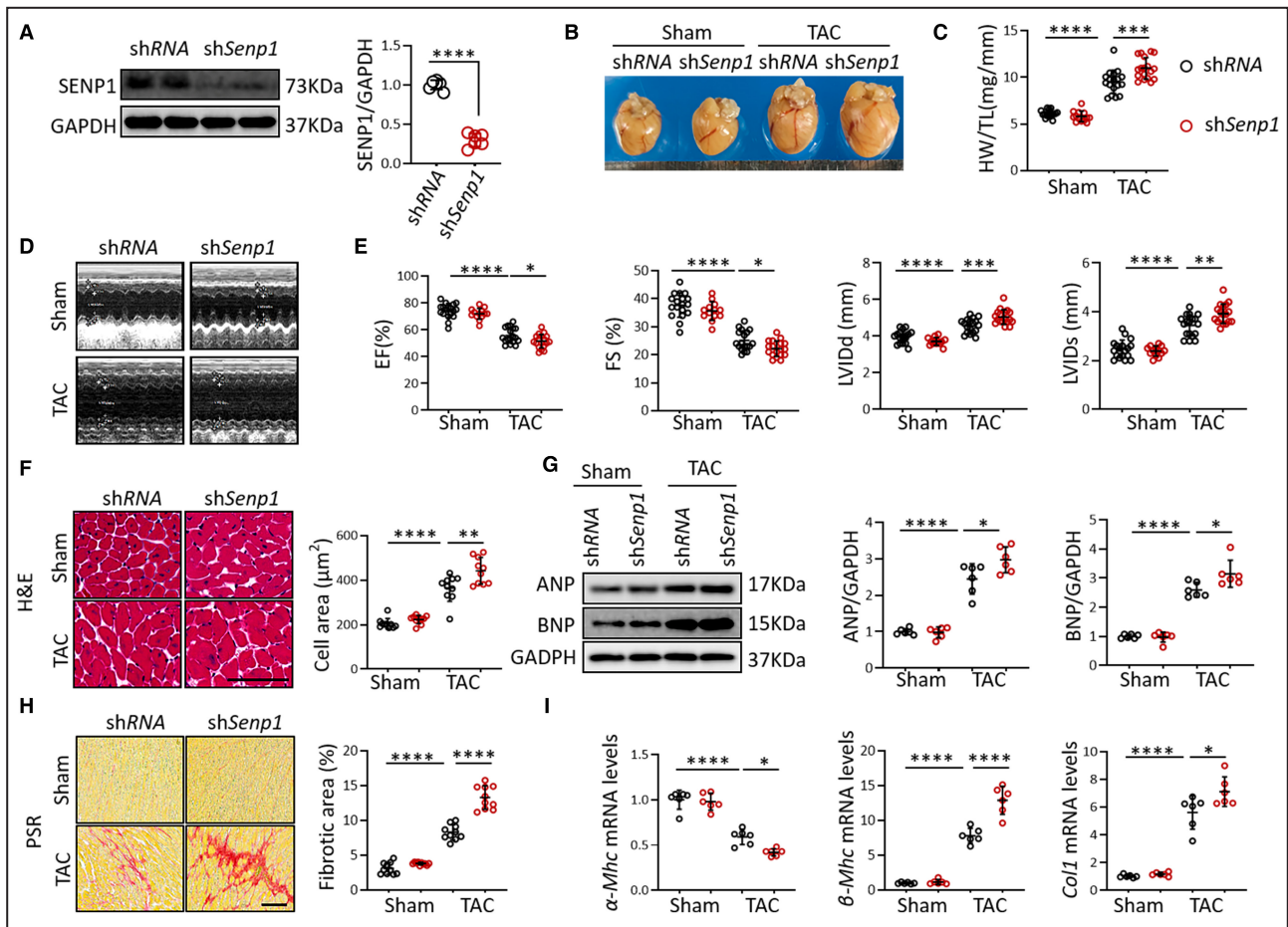


**Figure 2. SENP1 (Sentrin/small ubiquitin-like modifier-specific protease 1) deficiency aggravates pressure overload-induced cardiac remodeling and dysfunction.**

**A**, Representative western blot analysis and quantitative data for SENP1 protein levels in mouse hearts transduced with adeno-associated virus serotype 9-short hairpin RNA (shRNA) or adeno-associated virus serotype 9-shSenp1 (n=6 per group). Protein expression was quantified and normalized to GAPDH. **B**, Representative images of heart tissues isolated from shRNA sham, shSenp1 sham, shRNA transverse aortic constriction (TAC), and shSenp1 TAC mice. **C**, The ratios of heart weight to tibia length were calculated in shRNA or shSenp1 treated mice following 4 weeks of sham or TAC operations (n=18 for shRNA sham, shRNA TAC and shSenp1 TAC groups; n=13 for shSenp1 sham group). **D**, Representative M-mode images of shRNA sham, shSenp1 sham, shRNA TAC, and shSenp1 TAC mice. **E**, Echocardiographic quantification of ejection fraction, fractional shortening, left ventricular internal dimension diastolic, and left ventricular internal dimension systolic in the indicated groups (n=18 for shRNA sham, shRNA TAC and shSenp1 TAC groups; n=13 for shSenp1 sham group). **F**, Hematoxylin & eosin staining and quantitative data for cardiac cross-sections from shRNA- or shSenp1-treated mice following 4 weeks of sham or TAC operations (n=10 per group). Scale bar, 100 µm. **G**, Representative western blots and quantitative data for ANP and BNP protein levels in the indicated groups (n=6 per group). Protein expression was quantified and normalized to GAPDH. **H**, Representative Picrosirius red staining and quantitative data for cardiac fibrotic areas in shRNA- or shSenp1-treated mice following 4 weeks of sham or TAC operations (n=10 per group). Scale bar, 100 µm. **I**, Quantitative polymerase chain reaction analysis of hypertrophic and fibrotic gene expression in the indicated groups (n=6 per group). mRNA expression was quantified and normalized to GAPDH. Values represent the mean±SD. Statistical analysis was done using unpaired Student *t*-test (**A**) and 2-way ANOVA with Bonferroni post hoc test for panels (**C**, **E** through **I**). α-Mhc indicates α-myosin heavy chain; β-Mhc, β-myosin heavy chain; ANP, atrial natriuretic peptide; BNP, brain natriuretic peptide; Col1, collagen type I; EF, ejection fraction; FS, fractional shortening; H&E, hematoxylin and eosin; HW, heart weight; SENP1, Sentrin/small ubiquitin-like modifier-specific protease 1; shRNA, short hairpin RNA; TAC, transverse aortic constriction; and TL, tibia length. \**P*<0.05; \*\**P*<0.01; \*\*\**P*<0.001; \*\*\*\**P*<0.0001.

Picrosirius red revealed that the collagen contents in AAV9-shSenp1 mice were markedly increased compared with AAV9-shRNA mice at 4 weeks after TAC surgery (Figure 2H). Simultaneously, the mRNA levels of some markers of cardiac hypertrophy and fibrosis including α-MHC, β-MHC, and Col1 (collagen

type I) were also measured, qRT-PCR data showed that SENP1 depletion aggravated TAC-induced hypertrophic and fibrotic response (Figure 2I). These loss-of-function data collectively indicated that SENP1 depletion deteriorated pressure overload-induced cardiac pathological remodeling and dysfunction.

## SENP1 Overexpression Alleviates Pressure Overload-Induced Cardiac Remodeling and Dysfunction

Considering that SENP1 deficiency deteriorated hypertrophic response and aggravated cardiac function post-TAC, we then assessed the contribution of exogenous supplementation of SENP1 in pressure-overload cardiac hypertrophy. In this set of experiments, male C57BL/6 mice were first infected with AdSenp1 or AdGfp and then distributed to TAC or sham operations 1 week later. These mice were followed up for 4 more weeks before being euthanized. Figure S2C demonstrated that the adenoviruses were successfully transduced into the myocardium, and SENP1 levels in the myocardium were significantly increased compared with the AdGfp-transduced group (Figure S2D). Notably, the molecular, histological, and functional analysis demonstrated that cardiac hypertrophy and dysfunction induced by TAC were markedly attenuated in mice that received exogenous SENP1. Cardiac functional assessment via echocardiogram demonstrated that pressure overload significantly increased left ventricular internal dimension diastolic and left ventricular internal dimension systolic but decreased left ventricular ejection fraction and left ventricular fractional shortening, however, SENP1 overexpression markedly attenuated cardiac dysfunction induced by pressure overload (Figure 3A). SENP1-overexpressed mice also exhibited smaller gross size of hearts and decreased heart weight to tibia length ratios in response to pressure overload compared with the control mice (Figure 3B and 3C). In accordance with these findings, results obtained from wheat germ agglutinin staining indicated that TAC-induced cardiomyocyte hypertrophy was greatly improved in mice with SENP1 overexpressed (Figure 3D). Experimental results obtained from qRT-PCR also revealed that SENP1 overexpression effectively blocked TAC-induced hypertrophic response, as indicated by reduced ANP, BNP, and  $\beta$ -MHC levels but increased  $\alpha$ -MHC expression (Figure 3E). Moreover, Picosirius red staining suggested that the induction of fibrotic response by TAC was mitigated in SENP1 overexpression group (Figure 3F). The levels of fibrotic markers including Col1 and Col3 were lower in hypertrophic hearts with SENP1 overexpressed (Figure 3G). Collectively, these results revealed that SENP1 protected against pressure overload-induced cardiac remodeling and dysfunction.

## SENP1 Has No Effects On Cardiac Inflammation Induced By Pressure Overload

Inflammatory response acts as another significant characteristic during chronic pressure overload. We

next evaluated the impact of SENP1 on cardiac inflammation. Immunohistochemistry staining of CD45 and CD68 indicated that TAC led to the increased cardiac inflammatory response. Interestingly, no significant differences were observed in hypertrophic murine hearts with SENP1 ablation or overexpression compared with their control groups (Figure S3A and S3B). These data suggested that SENP1 had no effects on cardiac inflammatory response induced by chronic pressure overload.

## SENP1 Protects the Heart from Apoptosis During Pressure Overload

It has been reported that SENP1 profoundly affected I/R injury-induced cardiomyocyte apoptosis.<sup>10</sup> To further define whether SENP1 had an effect on pressure overload-induced cellular apoptosis, the protein levels of Bax and Bcl-2 were detected. Experimental results illustrated that TAC induced a remarkable elevation in Bax expression but a decrease in Bcl-2 expression compared with sham control, however, SENP1 depletion aggravated while SENP1 overexpression mitigated apoptotic response during pressure overload (Figure S3C and S3D).

## SENP1 Deficiency Is Associated With Increased STAT3 Phosphorylation

The prominent effects of SENP1 on pressure overload-induced cardiac hypertrophy and dysfunction prompted us to explore the underlying mechanisms. A set of documented studies have demonstrated that some key regulators potentially involved in cardiac hypertrophy may act as the direct targets of SENP1. For instance, SENP1 was capable of stabilizing HIF1 $\alpha$  during the hypoxic response.<sup>10,23</sup> Moreover, SENP1 could modulate the expression level as well as the nucleoplasmic distribution of Sirt1 to suppress its deacetylase activity in hyperoxic lung injury.<sup>24</sup> There also existed studies revealing that the SENP1-Sirt3 axis participated in the regulation of mitochondrial metabolism.<sup>25,26</sup> Additionally, PTEN may act as an essential target of SENP1 in the progress of tumorigenesis.<sup>27</sup> Thus, we first evaluated whether these target proteins were involved in SENP1-regulated hypertrophic response. Results from immunoblotting showed the significantly elevated levels of HIF1 $\alpha$  and P-AKT, and reduced levels of PTEN, Sirt1, and Sirt3 induced by hypertrophic stress, however, no significant alterations in these protein levels after either SENP1 depletion or overexpression were observed (Figure S4A and S4B). Moreover, previous studies have illustrated that the depletion of SENP1 suppressed lipopolysaccharide-induced macrophage inflammation by regulating the expression of inflammatory cytokines interleukin-6 (IL-6), indicating that inflammatory factors were potential downstream



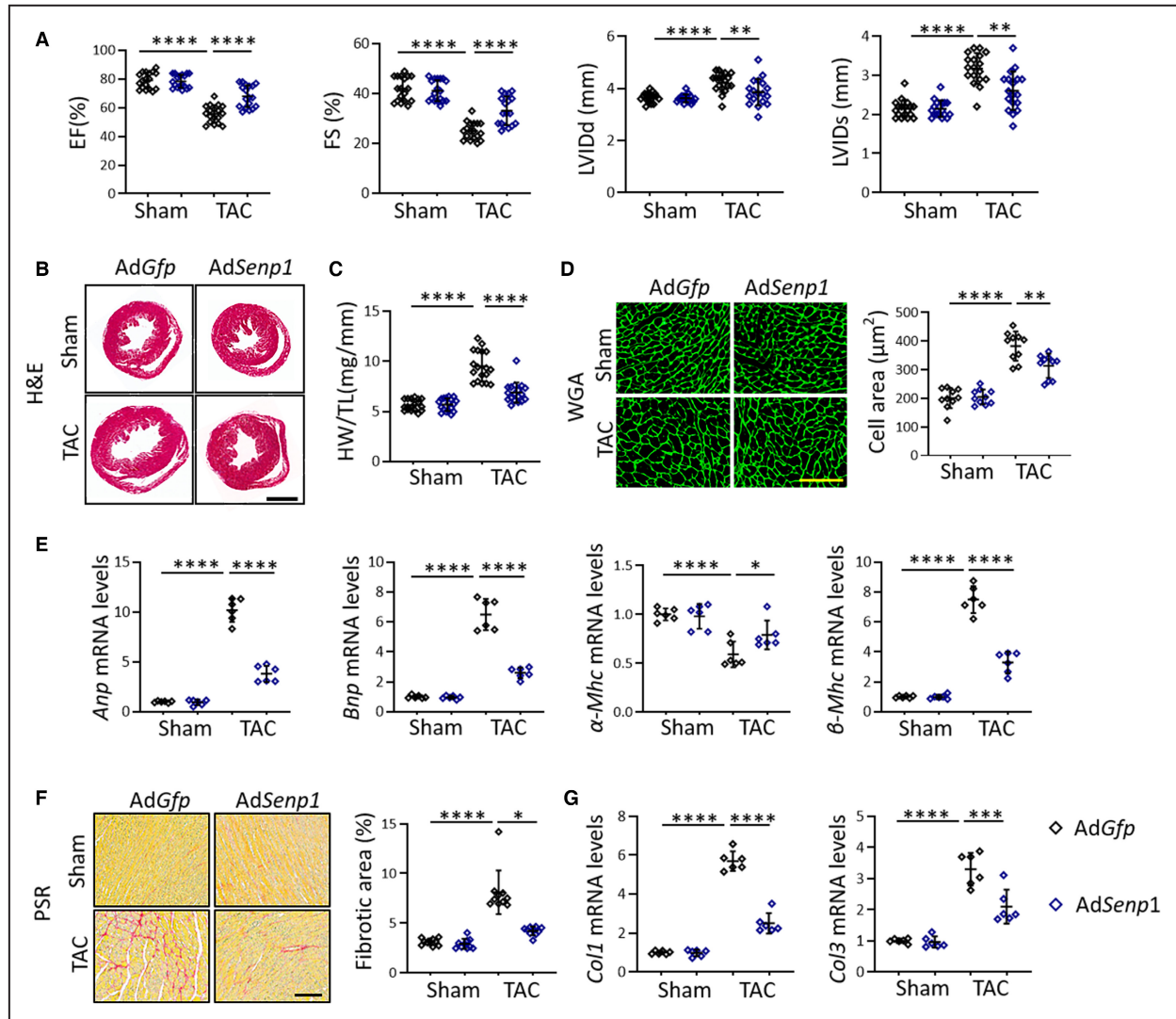


**Figure 3. SENP1 (Sentrin/small ubiquitin-like modifier-specific protease 1) overexpression mitigates pressure overload-induced cardiac remodeling and dysfunction.**

**A**, Echocardiographic quantification of ejection fraction, fractional shortening, left ventricular internal dimension diastolic, and left ventricular internal dimension systolic in *AdGfp* sham, *AdSenp1* sham, *AdGfp* transverse aortic constriction (TAC), and *AdSenp1* TAC mice (n=18 per group). **B**, Histological sections of cardiac tissues from *AdGfp* or *AdSenp1* treated mice with sham or TAC surgery were stained with H&E. Scale bar, 2mm. **C**, The ratios of heart weight to tibia length were calculated in *AdGfp* or *AdSenp1* treated mice following 4 weeks of sham or TAC operations (n=18 per group). **D**, Representative images and quantitative data for wheat germ agglutinin-stained cardiac cross-sections in the indicated groups (n=10 per group). Scale bar, 100µm. **E**, qPCR analysis for hypertrophic gene expression in the indicated groups (n=6 per group). mRNA expression was quantified and normalized to GAPDH. **F**, Representative Picrosirius red staining and quantitative data for cardiac fibrotic areas in *AdGfp* or *AdSenp1* treated mice following 4 weeks of sham or TAC operations (n=10 per group). Scale bar, 100µm. **G**, qPCR analysis for fibrotic gene expression in the indicated groups (n=6 per group). mRNA expression was quantified and normalized to GAPDH. Values represent the mean±SD. All data were analyzed by 2-way ANOVA with Bonferroni post hoc test except panel F (Kruskal–Wallis).  $\alpha$ -Mhc indicates  $\alpha$ -myosin heavy chain;  $\beta$ -Mhc,  $\beta$ -myosin heavy chain; *Anp*, atrial natriuretic peptide; *Bnp*, brain natriuretic peptide; *Col1*, collagen type I; *Col3*, collagen type III; EF, ejection fraction; FS, fractional shortening; GFP, green fluorescence protein; H&E, hematoxylin and eosin; LVIDd, left ventricular internal dimension diastolic; LVIDs, left ventricular internal dimension systolic; SENP1, Sentrin/small ubiquitin-like modifier-specific protease 1; TAC, transverse aortic constriction; and WGA, wheat germ agglutinin. \* $P$ <0.05; \*\* $P$ <0.01; \*\*\* $P$ <0.001; \*\*\*\* $P$ <0.0001.

targets of SENP1.<sup>28</sup> Interestingly, in the present study, we found that SENP1 had no effects on cardiac inflammatory response induced by chronic pressure overload. We thus asked whether SENP1 exerted its

profound roles via modulating the downstream targets of IL-6. Zhao et al<sup>29</sup> have revealed that IL-6 silencing significantly attenuated TAC-induced cardiac hypertrophy and markedly improved cardiac dysfunction by

manifesting STAT3 signaling, one of the most important downstream factors of IL-6. Multiple *in vivo* and *in vitro* studies have also implicated that STAT3 is constitutively activated by hypertrophic stress and interacts with a multitude of cellular and molecular mechanisms which modulate the progression of pressure overload-induced cardiac hypertrophy.<sup>29–31</sup>

Therefore, we asked whether the aggravation of pre-established cardiac hypertrophy after SENP1 silencing might be attributed to the altered activity of STAT3. Utilizing immunoblotting-based approaches, we detected distinct phosphorylation of STAT3 following TAC operation, and surprisingly, STAT3 phosphorylation levels were markedly elevated in SENP1-deficient hypertrophic mouse hearts (Figure 4A and 4B). Considering that JAK2 acts as a key upstream regulatory factor and is responsible for signaling transduction in various cellular processes through STAT3,<sup>32</sup> we also detected JAK2 phosphorylation and found that the phosphorylated JAK2 (P-JAK2) levels were markedly enhanced in SENP1-deficient hypertrophic murine hearts compared with those receiving AAV9-shRNA (Figure 4A and 4B). Conversely, the JAK2/STAT3 signaling cascade was inhibited in AdSenp1 mice compared with the AdGfp group in response to hypertrophic stress (Figure 4A and 4B). To further verify the effects of SENP1 on STAT3 signaling, we treated cultured NRCMs with AdshSenp1 or AdSenp1 to downregulate or upregulate SENP1 expression, and western blots confirmed that the levels of SENP1 were significantly changed (Figure S5A and S5B). Consistent with the *in vivo* results, the *in vitro* experimental data illustrated that SENP1 deletion strengthened the levels of P-JAK2 and P-STAT3 in phenylephrine-treated NRCMs, whereas SENP1 overexpression weakened the phosphorylation levels of JAK2 and STAT3 in response to phenylephrine stimulation (Figure 4C and 4D). In NRCMs, STAT3 inhibition diminished the detrimental effects of SENP1 deficiency on hypertrophic response as indicated by the decreased cellular size and mRNA levels of ANP and  $\beta$ -MHC (Figure 4E and 4F). Thus, these results suggested that the cardioprotective roles of SENP1 against pressure overload-induced cardiac hypertrophy may attribute to STAT3 signaling.

### SENP1 Modulates the Nuclear Translocation of STAT3

STAT3, distributed in the cytoplasm in an inactive form, is rapidly and transiently activated by a range of pathological stimuli. The activation of STAT3 and subsequent dimer formation trigger the nuclear translocation of STAT3 to drive the transcription of target genes.<sup>33</sup> Thus, we further examined the effects of SENP1 on the nuclear translocation of STAT3 in NRCMs treated by hypertrophic stress. Phenylephrine

treatment significantly increased STAT3 phosphorylation and nuclear STAT3 levels compared with control. Notably, SENP1 depletion promoted STAT3 phosphorylation and subsequent nuclear translocation, in contrast, SENP1 overexpression markedly prevented the activation and nuclear translocation of STAT3 in response to phenylephrine treatment (Figure 5A and 5B). Consistent with these findings, results from immunofluorescence staining revealed that, P-STAT3 expression was induced in NRCMs stimulated with phenylephrine and localized in the nucleus. However, SENP1 ablation led to a significant increase in nuclear P-STAT3 levels while SENP1 overexpression resulted in decreased nuclear P-STAT3 expression in response to phenylephrine (Figure 5C and 5D). In summary, these results indicated that SENP1 prevented the nuclear translocation of STAT3 to regulate the hypertrophic response.

### SENP1 Can Interact With JAK2/STAT3 Signaling

To further investigate the effect of SENP1 on the STAT3-associated signaling in hypertrophic response, we performed immunoprecipitation with anti-JAK2 or anti-STAT3 antibodies followed by immunoblot with anti-SENP1 antibody. As shown in Figure 6A and 6B, in lysis isolated from both murine heart tissues and NRCMs, JAK2 or STAT3 could interact with SENP1. To validate the protein–protein interaction of SENP1 and JAK2/STAT3, co-immunofluorescence of SENP1 and JAK2 or STAT3 in cultured myocyte cells was also performed to visually detect their relationships, and the results showed that JAK2 or STAT3 co-localized with SENP1 in cellular compartments (Figure 6C and 6D). These results implied that SENP1 could interact with JAK2 or STAT3 in phenylephrine-treated NRCMs, which subsequently regulate the activation of STAT3.

### Cardiomyocyte-Specific Deletion of STAT3 Negates the Detrimental Effects of SENP1 Deficiency on Cardiac Hypertrophy

Based on the above observations, we performed *in vitro* experiments using cultured NRCMs and H9c2 cells to test whether the cardioprotective roles of SENP1 in cardiac hypertrophy were STAT3-dependent. Cultured cells were treated by AdshSenp1 as well as siStat3, and then stimulated by phenylephrine. Immunoblotting and immunofluorescence results confirmed the successful depletion of STAT3 in cultured cells (Figure S5C and S5D). In hypertrophic NRCMs, inhibition of STAT3 markedly diminished the increase in cellular size and mRNA levels of ANP and  $\beta$ -MHC (Figure 4E and 4F). Similar results were also obtained in H9c2 cells (Figure S6A through S6D). To further identify the causal

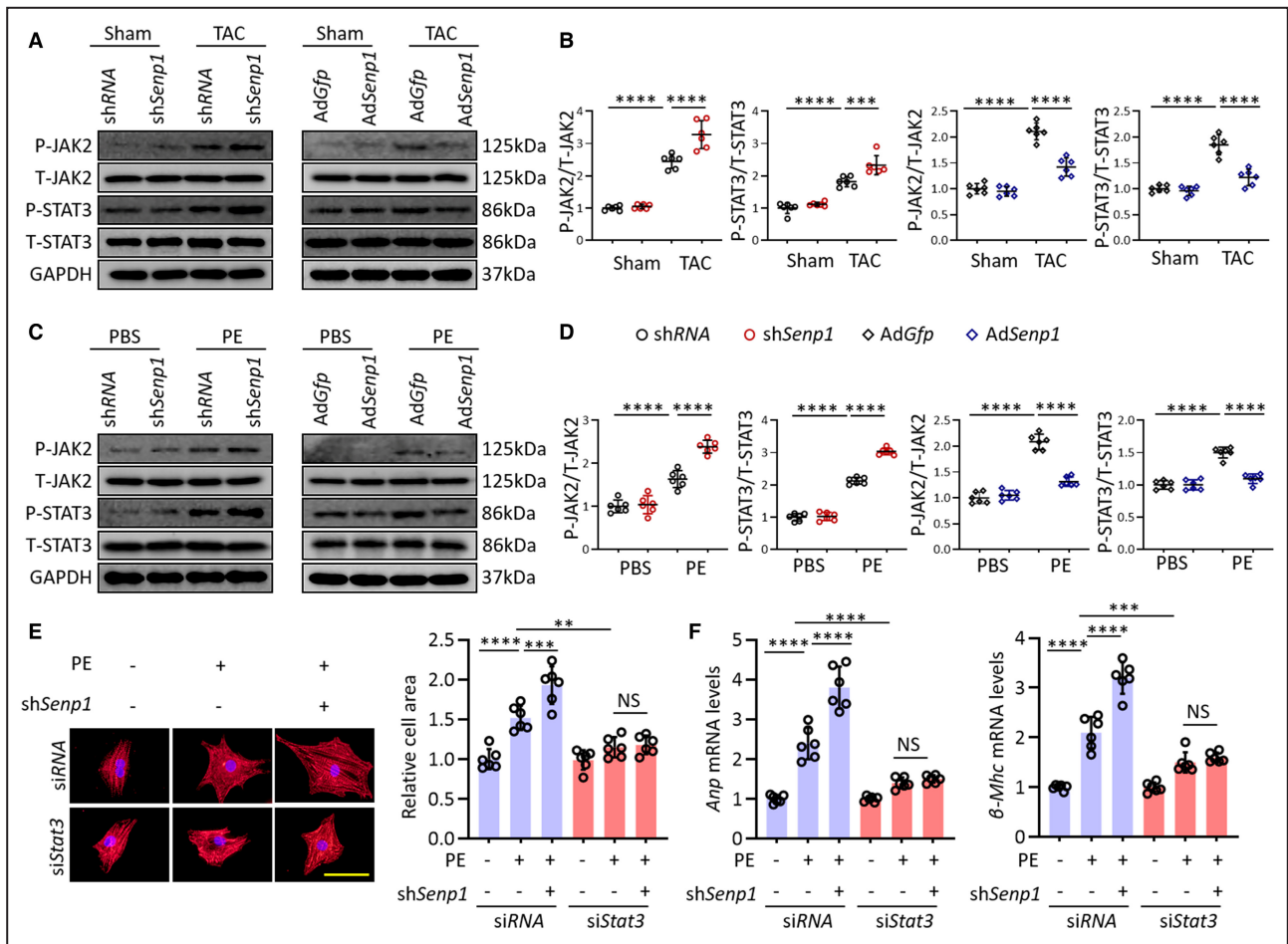


**Figure 4. STAT3 signaling is the downstream of SENP1 (Sentrin/small ubiquitin-like modifier-specific protease 1) in the regulation of pressure overload-induced cardiac hypertrophy and dysfunction.**

**A**, Representative western blot analysis of phosphorylated JAK2 (P-JAK2), JAK2, P-STAT3, and STAT3 protein levels in cardiac extracts from mice in the indicated groups (n=6 per group). Protein expression was quantified and normalized to GAPDH. **B**, Quantification of protein expression in the indicated groups based on the western blots in A. **C**, Representative western blot analysis of P-JAK2, JAK2, P-STAT3, and STAT3 protein levels from neonatal rat cardiomyocytes in the indicated groups (n=6 independent experiments). Protein expression was quantified and normalized to GAPDH. **D**, Quantification of protein expression in the indicated groups based on the western blots in C. **E**, Representative images and quantitative data for immunofluorescence staining of  $\alpha$ -actinin in neonatal rat cardiomyocytes in the indicated groups (n=6 independent experiments). Scale bar, 50  $\mu$ m. **F**, Quantitative polymerase chain reaction analysis for hypertrophic gene expression in neonatal rat cardiomyocytes in the indicated groups (n=6 independent experiments). mRNA expression was quantified and normalized to GAPDH. Values represent the mean  $\pm$  SD. All data were analyzed by 2-way ANOVA with Bonferroni post hoc test. Ad indicates adenoviral; *Anp*, atrial natriuretic peptide; GFP, green fluorescence protein; JAK2, Janus kinase 2;  $\beta$ -Mhc,  $\beta$ -myosin heavy chain; NS, not significant; P, phosphorylated; SENP1, Sentrin/small ubiquitin-like modifier-specific protease 1; shRNA, short hairpin RNA; STAT3, signal transducer and activator of transcription 3; and T, total. \* $P$ <0.05; \*\* $P$ <0.01; \*\*\* $P$ <0.001; \*\*\*\* $P$ <0.0001.

association between STAT3 signaling and SENP1-regulated cardiac hypertrophy, we utilized an inducible Cre-dependent system to deplete STAT3 in cardiomyocytes. Specifically, we generated *Stat3* conditional knockout mice by crossing *Stat3*-floxed mice with mice carrying the  $\alpha$ MHC-MCM transgene (Figure S7A). We performed the genotypic identification of *Stat3* conditional knockout mice by polymerase chain reaction using genomic DNA isolated from murine toes. The polymerase chain reaction primer sequences of *Stat3*-floxed mice are: 5'-TTGACCTGTGCTCCTACAAAA-3'

and 5'-CCCTAGATTAGGCCAGCACA-3'. The wild-type allele was shown to 146bp, the mutant allele 187bp, and the heterozygote allele generated both 146 and 187bp bands (Figure S7B). The  $\alpha$ MHC-MCM mice were genotyped according to the following primer sequences: 5'-AGGTGGACCTGATCATGGAG-3', 5'-ATACCGGAGATCATGCAAGC-3', 5'-CTAGGCCACAGAATGAAAAGATCT-3', and 5'-GTAGGTGGAAATTCTGCATCATCC-3'. These cross-bred *STAT3*<sup>fllox/fllox</sup>; $\alpha$ MHC-MCM mice and their negative controls were then intraperitoneally injected with tamoxifen (25mg/kg, for

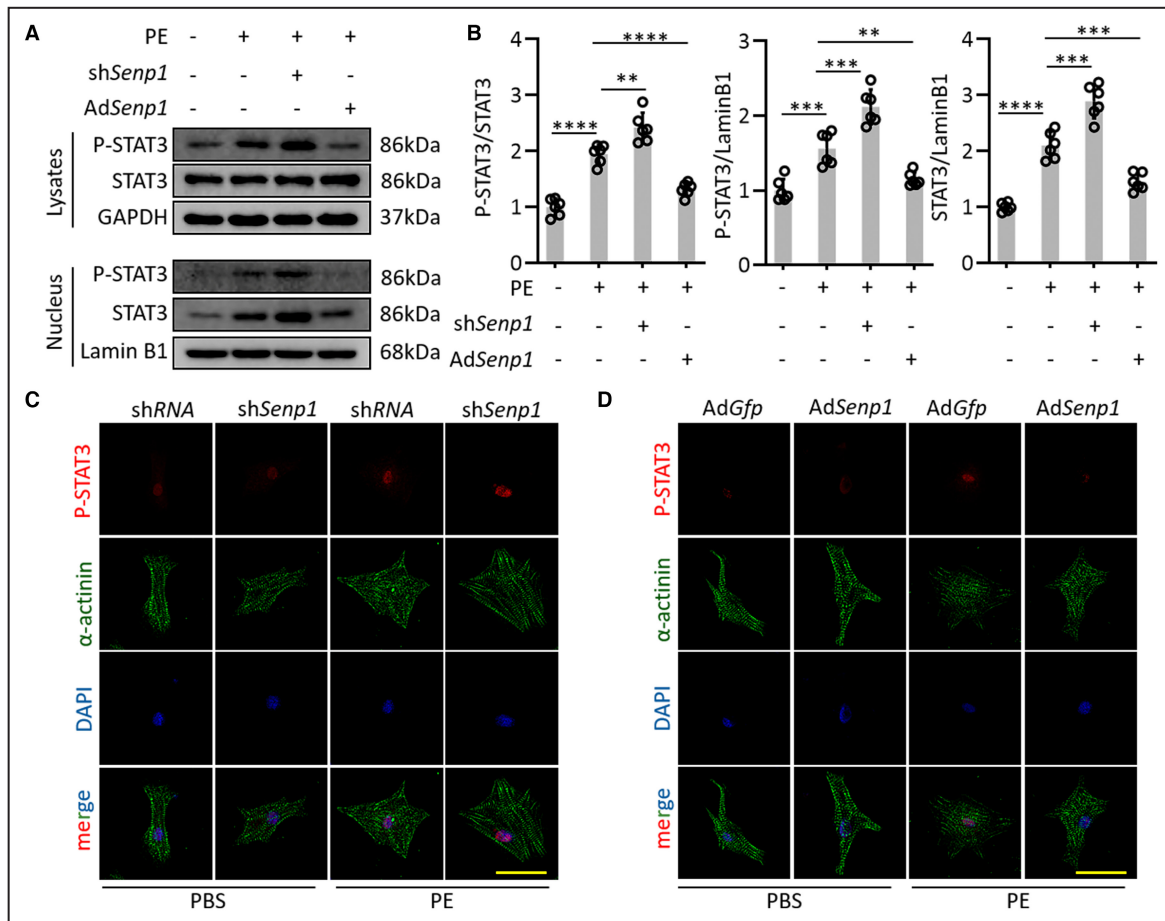


**Figure 5. SENP1 (Sentrin/small ubiquitin-like modifier-specific protease 1) modulates the nuclear translocation of STAT3 in response to hypertrophic stimuli.**

**A**, Representative western blot analysis of whole-cell and nuclear contents of P-STAT3 and STAT3 proteins from neonatal rat cardiomyocytes in the indicated groups (n=6 independent experiments). Protein expression was normalized to GAPDH and Lamin B1, respectively. **B**, Quantitative data for whole-cell and nuclear contents of P-STAT3 and STAT3 based on the western blots in **A**. **C**, Representative images for immunofluorescence staining of  $\alpha$ -actinin (green) and P-STAT3 (red) in neonatal rat cardiomyocytes treated with shRNA or shSenp1 plus phenylephrine (50  $\mu$ mol/L) or vehicle. Scale bar, 50  $\mu$ m. **D**, Representative images for immunofluorescence staining of  $\alpha$ -actinin (green) and P-STAT3 (red) in neonatal rat cardiomyocytes treated with AdGfp or AdSenp1 plus phenylephrine (50  $\mu$ mol/L) or vehicle. Scale bar, 50  $\mu$ m. Values represent the mean $\pm$ SD. All data were analyzed by 1-way ANOVA with Bonferroni post hoc test. Ad indicates adenoviral; DAPI, 4',6-diamidino-2-phenylindole; P, phosphorylated; SENP1, Sentrin/small ubiquitin-like modifier-specific protease 1; shRNA, short hairpin RNA; and STAT3, signal transducer and activator of transcription 3. \* $P$ <0.05; \*\* $P$ <0.01; \*\*\* $P$ <0.001; \*\*\*\* $P$ <0.0001.

5 consecutive days) to induce cardiomyocyte-specific STAT3 deletion (Figure S7A). Subsequently, the animals underwent intravenous injection to downregulate SENP1 expression, and finally were subjected to TAC or sham operations. Results from immunoblotting showed that STAT3 levels were downregulated in Stat3 conditional knockout murine hearts compared with controls (Figure S7C). As expected, the histological analysis suggested that cardiomyocyte-specific ablation of STAT3 could diminish the difference of cardiac hypertrophy between mice receiving AAV9-shRNA and AAV9-shSenp1 (Figure 7A-C). Additionally, the cardiac function was significantly ameliorated by

cardiomyocyte-specific STAT3 silencing in both AAV9-shRNA and AAV9-shSenp1 treated mice subjected to TAC (Figure 7D). The mRNA levels of some hypertrophic markers also tended to be normal when STAT3 was depleted (Figure 7E). These results indicated that the effects of SENP1 on pressure overload-induced cardiac hypertrophy were STAT3-dependent.

Next, we asked whether the modulatory roles of SENP1 were dependent on JAK2/STAT3 signaling. We treated SENP1-depleted hypertrophic NRCMs with some inhibitors targeting STAT3-associated signaling, including LLY-507 (Smyd2 inhibitor), ACY-1215 (HDAC6 inhibitor), AG825 (ErbB2 inhibitor), and AG490 (JAK2

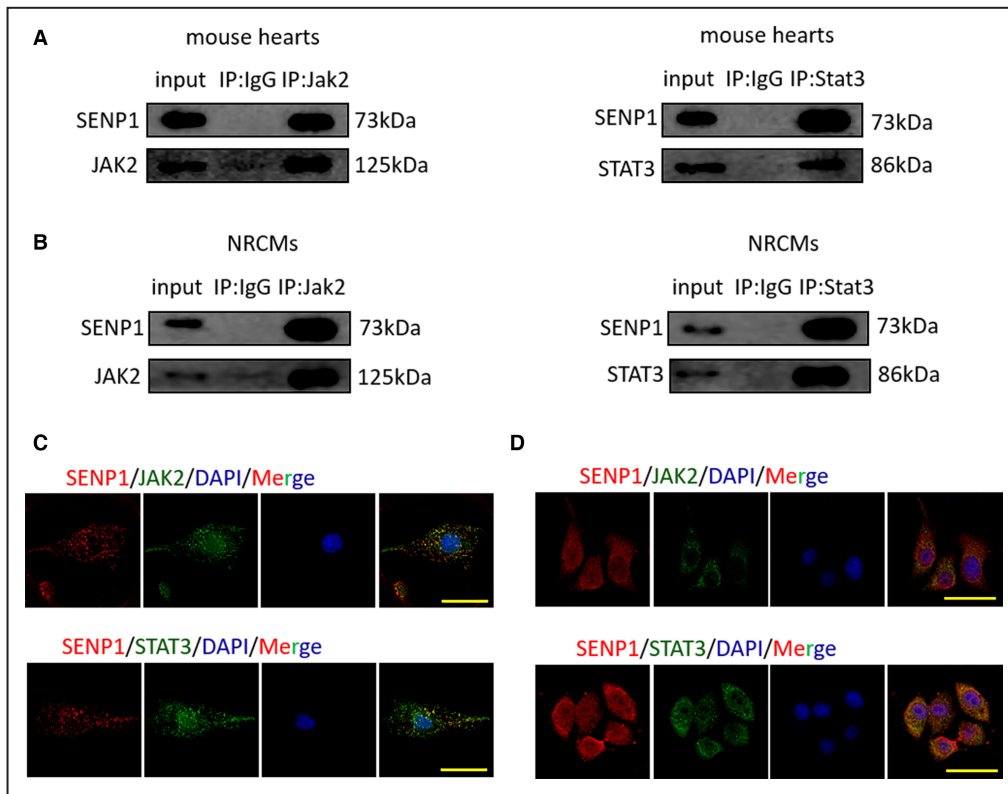


**Figure 6. SENP1 (Sentrin/small ubiquitin-like modifier-specific protease 1) can interact with JAK2/STAT3 signaling.**

**A**, Representative images for western blotting for SENP1 and JAK2 in myocardial tissues from transverse aortic constriction-treated mice immunoprecipitated with anti-JAK2 antibody (left). Anti-STAT3 immunoprecipitates were immunoblotted with anti-SENP1 and anti-STAT3 antibody (right). **B**, Representative images for western blotting for SENP1 and JAK2 in phenylephrine-treated neonatal rat cardiomyocytes immunoprecipitated with anti-JAK2 antibody (left). Anti-STAT3 immunoprecipitates were immunoblotted with anti-SENP1 and anti-STAT3 antibody (right). **C**, Representative images for immunofluorescence staining of JAK2 (green)+SENP1 (red) (top) or STAT3 (green)+SENP1 (red) (bottom) in neonatal rat cardiomyocytes treated with phenylephrine. Scale bar, 50  $\mu$ m. **D**, Representative images for immunofluorescence staining of JAK2 (green)+SENP1 (red) (top) or STAT3 (green)+SENP1 (red) (bottom) in H9c2 cells treated with phenylephrine. Scale bar, 50  $\mu$ m. DAPI indicates 4',6-diamidino-2-phenylindole; IgG, immunoglobulin G; JAK2, Janus kinase 2; NRCMs, neonatal rat cardiomyocytes; SENP1, Sentrin/small ubiquitin-like modifier-specific protease 1; and STAT3, signal transducer and activator of transcription 3.

inhibitor). As expected, only in the NRCMs treated with JAK2 inhibitor AG490, STAT3 phosphorylation levels and the hypertrophic response were prevented (Figure S8A through S8C). Taken together, these results indicated that the potential cardioprotective effects of SENP1 were dependent on JAK2/STAT3 signaling in cardiomyocytes.

### Pharmacological Inhibition of SENP1 by Momordin Ic Accelerates Pressure Overload-Induced Cardiac Remodeling

Previous studies have demonstrated that SENP1 plays essential roles in the occurrence, development

and metastasis of various tumors, and suppressing SENP1 expression has become a goal for cancer treatments.<sup>34,35</sup> Giving the detrimental role of SENP1 loss in cardiac hypertrophy, systemic SENP1 inhibition may bring side effects on the heart. Mc, a pentacyclic triterpene extracted from multiple Chinese natural medicines, has been proved to be a new natural SENP1 inhibitor and exert obvious antitumor effects.<sup>14</sup> Thus, we treated mice with Mc to determine the roles of pharmacological SENP1 inhibition in TAC-induced cardiac remodeling. Notably, administration of Mc aggravated TAC-induced cardiac hypertrophic response, with markedly increased heart weight to tibia length ratios and cardiomyocyte cross-sectional

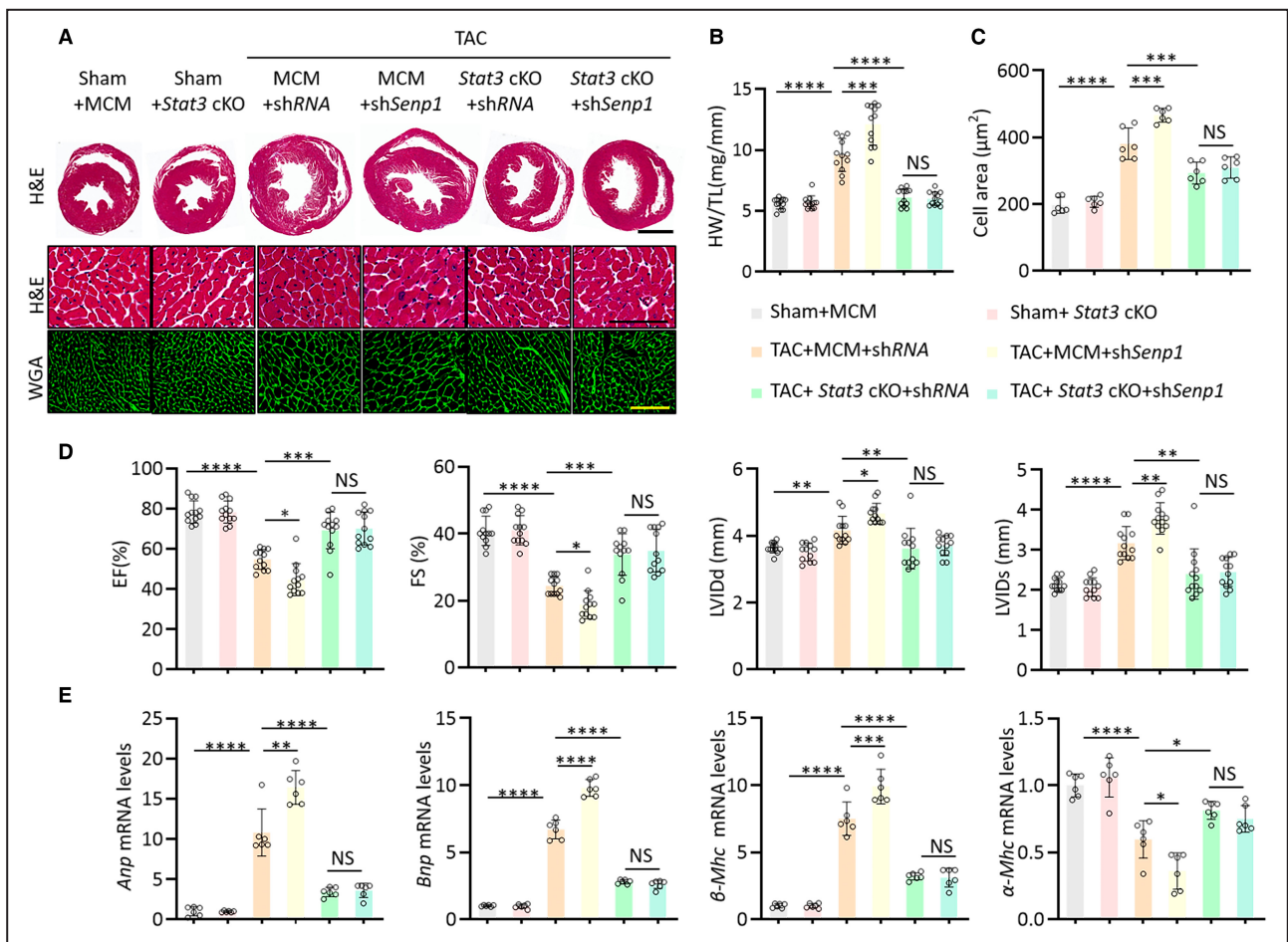


**Figure 7. Cardiomyocyte-specific deletion of STAT3 negates the detrimental effects of SENP1 (sentrin/small ubiquitin-like modifier-specific protease 1) deficiency on cardiac hypertrophy.**

**A**, Representative images of hematoxylin and eosin and wheat germ agglutinin-stained cardiac cross-sections in the indicated groups. Scale bar, 2mm (top), 100µm (middle and bottom). **B**, The ratios of heart weight to tibia length were calculated in the indicated groups (n=12 per group). **C**, Quantitative data for cell areas based on hematoxylin and eosin staining in A (n=6 per group). **D**, Echocardiographic quantification of ejection fraction, fractional shortening, left ventricular internal dimension diastolic, and left ventricular internal dimension systolic in the indicated groups (n=12 per group). **E**, qPCR analysis for hypertrophy-associated gene expression in the indicated groups (n=6 per group). mRNA expression was quantified and normalized to GAPDH. Values represent the mean±SD. All data were analyzed by 2-way ANOVA with Bonferroni post hoc test. α-MHC indicates α-myosin heavy chain; β-MHC, β-myosin heavy chain; *Anp*, atrial natriuretic peptide; *Bnp*, brain natriuretic peptide; cKO, conditional knockout; EF, ejection fraction; FS, fractional shortening; H&E, hematoxylin and eosin; HW, heart weight; LVIDd, left ventricular internal dimension diastolic; LVIDs, left ventricular internal dimension systolic; MCM, MerCreMer; NS, not significant; SENP1, Sentrin/small ubiquitin-like modifier-specific protease 1; shRNA, short hairpin RNA; STAT3, signal transducer and activator of transcription 3; TAC, transverse aortic constriction; TL, tibia length; and WGA, wheat germ agglutinin. \**P*<0.05; \*\**P*<0.01; \*\*\**P*<0.001; \*\*\*\**P*<0.0001.

areas (Figure 8A through 8C). Hypertrophic markers including ANP and BNP were also elevated in Mc-treated mice after 4 weeks of TAC (Figure 8D). Picrosirius red staining also revealed that the extent of cardiac fibrosis was significantly increased after Mc treatment (Figure 8E). qRT-PCR results showed that TAC-induced Col1 and Col3 (collagen type III) expression were markedly upregulated in the hearts isolated from Mc-treated mice (Figure 8F). These observations indicated that the administration of Mc aggravated cardiac remodeling induced by pressure overload.

## DISCUSSION

In this study, we have uncovered a previously unrecognized role of SENP1 in the setting of cardiac remodeling and dysfunction induced by chronic pressure overload. First, using different approaches, we observed that the mRNA and protein levels of SENP1 were augmented in heart tissues from a mouse model of TAC-induced cardiac injury as well as NRCMs treated by pro-hypertrophic stimuli. By performing gain-of-function and loss-of-function animal experiments, we discovered a novel role of SENP1 in the

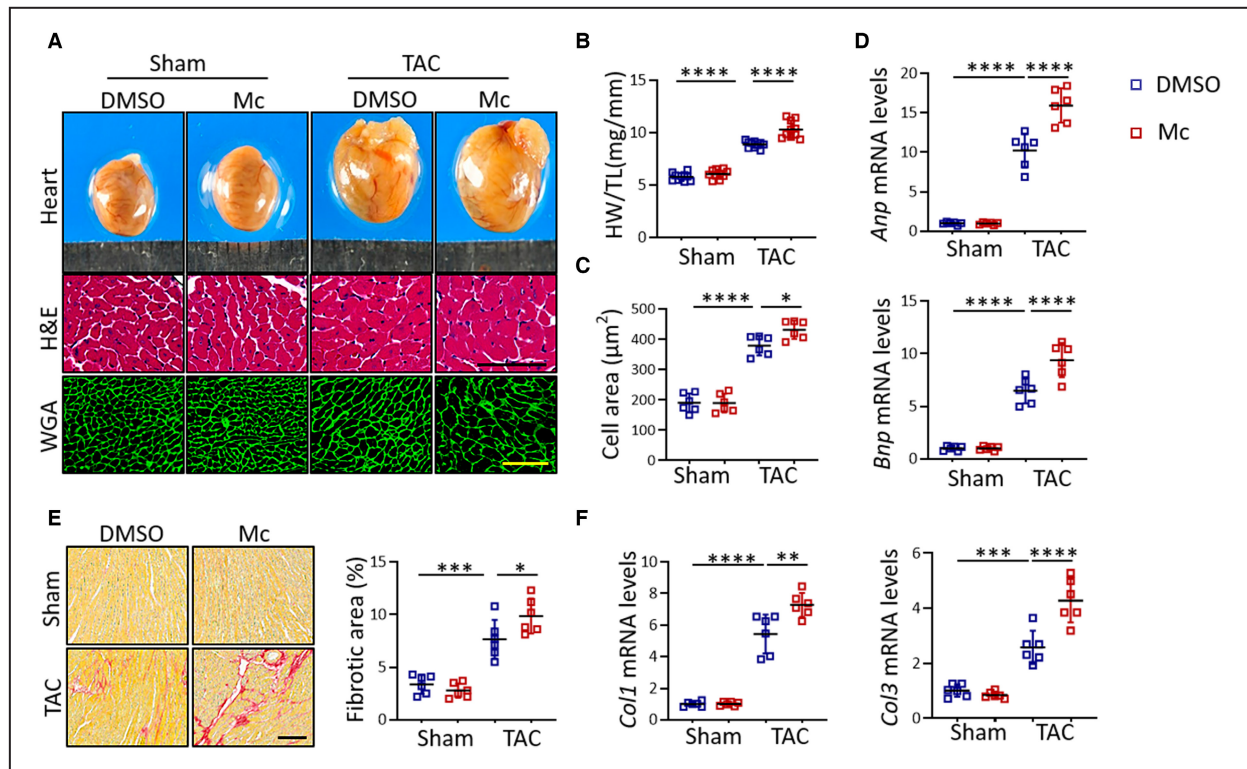


**Figure 8. Momordin Ic (Mc) accelerates pressure overload-induced cardiac remodeling.**

**A**, Representative images of heart tissues, hematoxylin and eosin staining, and wheat germ agglutinin staining in dimethyl sulphoxide sham, Mc sham, dimethyl sulphoxide transverse aortic constriction, and Mc transverse aortic constriction mice. Scale bar, 100  $\mu$ m. **B**, The ratios of heart weight to tibia length were calculated in dimethyl sulphoxide or Mc-treated mice following 4 weeks of sham or transverse aortic constriction operations (n=10 per group). **C**, Quantitative data for cell areas based on hematoxylin and eosin staining in A (n=6 per group). **D**, Quantitative polymerase chain reaction analysis for ANP and BNP gene expression in the indicated groups (n=6 per group). mRNA expression was quantified and normalized to GAPDH. **E**, Representative Picrosirius red staining and quantitative data for cardiac fibrotic areas in dimethyl sulphoxide or Mc-treated mice following 4 weeks of sham or transverse aortic constriction operations (n=6 per group). Scale bar, 100  $\mu$ m. **F**, Quantitative polymerase chain reaction analysis for Col1 (collagen type I) and Col3 (collagen type III) gene expression in the indicated groups (n=6 per group). mRNA expression was quantified and normalized to GAPDH. Values represent the mean $\pm$ SD. All data were analyzed by 2-way ANOVA with Bonferroni post hoc test. *Anp* indicates atrial natriuretic peptide; *Bnp*, brain natriuretic peptide; *Col1*, collagen type I; *Col3*, collagen type III; DMSO, dimethyl sulphoxide; H&E, hematoxylin and eosin; HW, heart weight; Mc, Momordin Ic; TAC, transverse aortic constriction; TL, tibia length; and WGA, wheat germ agglutinin. \**P*<0.05; \*\**P*<0.01; \*\*\**P*<0.001; \*\*\*\**P*<0.0001.

pathogenesis of cardiac hypertrophy. The knock-down of SENP1 promoted TAC-induced hypertrophy and cardiac dysfunction; conversely, adenovirus-mediated overexpression of SENP1 in the myocardium protected against hypertrophic response and cardiac functional decline in a cardiac hypertrophy mouse model. Mechanically, SENP1 depletion in hypertrophic models led to increased phosphorylation of the JAK2/STAT3 signaling axis. Based on results from immunoprecipitation and immunoprecipitation, it was illustrated that SENP1 could interact with JAK2 as well as STAT3 and inhibit the activation and nuclear translocation of STAT3. In vivo experiments indicated that cardiomyocyte-specific knockout of STAT3 reverted the detrimental role of SENP1 ablation in mice subjected to TAC. Similar observations were also obtained from NRCMs treated with pro-hypertrophic stimuli.

SUMOylation has been well studied in the modulation of various cellular processes. Emerging evidence has shown that SUMOylation is an important reversible posttranslational modification that contributes to the maintenance of cardiac homeostasis during hypertrophic stimuli.<sup>36</sup> It has been illustrated that gene transfer-induced SUMO1 overexpression blocked the development of cardiac hypertrophy and failure in mice subjected to TAC via post-translational modifications of SERCA2a.<sup>37</sup> The SUMO1/SERCA2a signaling axis was also identified as an underlying mechanism of miR-146a regulation in failing cardiomyocytes.<sup>38</sup> Moreover, overexpression of UBC9, a SUMO E2 ligase, seemed to attenuate aggregate formation as well as cardiac hypertrophy through modulating cardiac autophagy in a murine model of proteotoxic cardiac disease.<sup>39</sup> These studies altogether illustrated that modulatory factors

in the process of SUMOylation may participate in the regulation of cardiac hypertrophy. Importantly, SENP1, a significant protease removing SUMOs from the modified proteins, is also expressed in the myocardium and plays profound roles in the heart. A documented study has reported that SENP1 exerted cardioprotective roles in I/R-induced cardiac acute injury via the hypoxia-inducible factor 1 alpha (HIF1 $\alpha$ )-dependent pathway.<sup>10</sup>

Cardiac hypertrophy represents a critical predisposing factor for cardiovascular events and heart failure, and the mechanisms involved are largely unknown. To date, the regulatory roles of SENP1 in pressure overload-induced cardiac hypertrophy and dysfunction remains unclear. By performing immunoblotting, we observed that SENP1 expression was significantly augmented in both hypertrophic hearts induced by chronic pressure overload and NRCMs treated with pro-hypertrophic stimuli. Moreover, results from immunostaining revealed that the upregulated SENP1 was expressed primarily in cardiomyocytes. Therefore, gain-of-function and loss-of-function experiments were performed to investigate the roles of SENP1 in pressure overload-induced cardiac hypertrophy. Our data supported SENP1 as a critical negative regulator during chronic pressure overload. Furthermore, previous studies have presented compelling evidence demonstrating that some critical regulators of cardiac hypertrophy such as HIF1 $\alpha$ , PTEN, Sirt1, and Sirt3 acted as downstream targets of SENP1.<sup>23–27</sup> Surprisingly, we observed no significant changes in these target proteins after SENP1 silencing or overexpression in cardiac hypertrophy. Therefore, these observations prompted us to propose other regulators potentially involved in this process.

Documented studies have illustrated that SENP1 ablation suppressed lipopolysaccharide-induced macrophage inflammation by regulating the expression of inflammatory cytokines IL-6, indicating that inflammatory factors were potential downstream targets of SENP1.<sup>28</sup> Interestingly, in the present study, we found that SENP1 had no effects on cardiac inflammatory response induced by chronic pressure overload. We thus asked whether SENP1 exerted its profound roles via modulating the downstream targets of IL-6. Previous studies have given evidence that the STAT3 signaling functions as a significant downstream regulator of IL-6 in various cellular processes, and importantly, knockout of IL-6 markedly attenuated TAC-induced cardiac hypertrophy and dysfunction via STAT3 signaling.<sup>29,33</sup> We thus asked whether the STAT3 signaling participated in SENP1-regulated cardiac hypertrophy. It has been well established that STAT3 serves as a significant contributor to the pathogenesis of cardiac hypertrophy. A multitude of cardiac stresses, such as pressure overload, neuro-hormones, cytokines,

epidermal growth factor, interferons, and hypertrophic agonists, can trigger a STAT3-associated signaling cascade.<sup>40</sup> It has also been well established that transgenic mice with cardiac-specific STAT3 overexpression manifested cardiac hypertrophy as indicated by the upregulation of hypertrophic markers and histological alterations,<sup>41</sup> while inhibiting the expression of STAT3 markedly suppressed cardiac hypertrophy and collagen synthesis.<sup>42</sup> Subsequent studies have also identified multiple factors, such as JAK2, IL-6, and gp130, that could positively or negatively regulate STAT3 expression during this process.<sup>29,43</sup> In addition, a number of studies have also pointed out that there exist therapeutic approaches which target STAT3 and are effective to prevent the progression of cardiac hypertrophy, suggesting that STAT3 may be a potential target for the treatment of cardiac hypertrophy.<sup>30,44,45</sup>

In the present study, we observed that SENP1 deficiency promoted the phosphorylation of STAT3 in an *in vivo* mouse TAC model and cultured NRCMs in parallel with the expression level of hypertrophic markers, indicating potential involvement of STAT3 in SENP1-mediated cardiac hypertrophy. We further confirmed that the SENP1-STAT3 axis modulated hypertrophic response using cardiomyocyte-specific STAT3 knockout mice as well as STAT3-depleted myocyte cells. These observations supported the notion that the STAT3-associated signaling axis might be an underlying mechanism in SENP1-mediated cardiac hypertrophy.

In addition, we also investigated the potential upstream regulator of STAT3 in this process. Results from immunoblotting revealed that SENP1 deficiency also augmented JAK2 phosphorylation *in vivo* and *in vitro*, which was in parallel with STAT3 phosphorylation. By performing immunofluorescence and immunoprecipitation in cultured myocyte cells, we discovered that SENP1 could interact with JAK2 as well as STAT3, and subsequently inhibit the activation and nuclear translocation of STAT3. Inhibition of JAK2 by AG490 significantly reversed STAT3 phosphorylation and cardiac hypertrophy in hypertrophic NRCMs deficient in SENP1. These data confirmed the potential involvement of the SENP1-JAK2-STAT3 signaling axis in cardiac hypertrophy induced by chronic pressure overload. Thus, we can conclude that the STAT3 signaling account for SENP1-mediated cardiac hypertrophy. Definitely, in addition to STAT3, there must be some other regulators which serve as the target proteins of SENP1 in the modulation of cardiac hypertrophy, and this work is of great interest and deserved further investigation.

Interestingly, a previous study has indicated that induction of SENP1 in myocardium was associated with cardiomyopathy and mitochondrial abnormalities,<sup>11</sup> which seemed to be contrary to our current findings. There exist some potential reasons for differences between observations in the present study and study by



Cai et al. First, SENP1 functions as an upstream modulator of diverse cellular signaling pathways,<sup>25,35,46</sup> thus manipulating on SENP1 expression may bring distinct changes to different signaling pathways. In the study by Cai et al,<sup>11</sup> they demonstrated that upregulation of SENP1 in myocardium gave rise to some mitochondrial-related genes and contributed to mitochondrial dysfunction. In the present study, we mainly focused on the modulatory roles of SENP1 in chronic pressure overload induced-hypertrophic response, which is characterized with cardiomyocyte enlargement, increased fibrosis, the upregulation of fetal genes, decreased contractility, and eventually heart failure.<sup>47,48</sup> And our study demonstrated the SENP1-JAK2-STAT3 regulatory axis involved in this process. As we know, cardiac hypertrophy is a decompensated consequence of the combined effect of multiple pathological factors, mitochondrial abnormalities only represents one aspect.<sup>1</sup> In addition, in the present study, we utilized gain- and loss-of-function method in mice subjected to TAC surgery to comprehensively analyze the effect of SENP1 in cardiac hypertrophy. Furthermore, our in vivo findings were further supported by observations in the vitro model of phenylephrine-induced cardiac hypertrophy, and the data altogether indicated a direct role of SENP1 in pressure overload-induced cardiac hypertrophy. Importantly, different types of cultured cells used in the 2 studies may also contribute to the discrepancy. In Cai's study, C2C12 myoblast cell line was used for mechanism exploration at cellular levels, while in the present study, NRCMs, a standard experimental in vitro system, were used for the investigation of cellular mechanisms in hypertrophic response.<sup>49,50</sup>

This study has several limitations. First, AAV9 delivery system was used in our study instead of the cardiomyocyte-specific knockout mice. Second, although we have demonstrated that SENP1 could directly bind to JAK2 and inhibit its phosphorylation, the detailed molecular relationship between SENP1 and activation of JAK2 requires further clarification.

In summary, the present study revealed that SENP1 expression was upregulated in both cardiac hypertrophic murine heart tissues and NRCMs challenged with hypertrophic stimuli. Aggravated cardiac hypertrophy and dysfunction were observed in mice deficient in SENP1. Conversely, exogenous overexpression of SENP1 suppressed TAC-induced cardiac remodeling. These observations indicated the cardioprotective roles in pressure overload-induced cardiac remodeling, which was in line with the protective roles of SENP1 against I/R. The regulatory effects of SENP1 in cardiac hypertrophy are mediated by STAT3-associated signaling. SENP1 could directly interact with JAK2 and STAT3 in cardiomyocytes, resulting in the inhibition of STAT3 activation and STAT3 nuclear translocation, thus bringing benefits to cardiac injury caused by chronic pressure overload. Our

data illustrated a new and previously unrecognized role of SENP1 in cardiac remodeling triggered by long-term pressure overload. Approaches to stimulate or stabilize SENP1 expression might be achieved to mitigate cardiac hypertrophy. In addition, our study has significant clinical implications. In the past decades, increasing number of studies have demonstrated the involvement of SENP1 in the tumorigenesis. And more importantly, some Food and Drug Administration-approved drugs were shown to target SENP1 and treat cancer, indicating the clinical value of SENP1 inhibitors in tumors.<sup>51</sup> Therefore, downregulation of SENP1 has become the goal of many cancer treatments. Mc, a new natural SENP1 inhibitor, has been shown to exert antitumor effects. However, in this study, we revealed that treatment with Mc aggravated TAC-induced cardiac remodeling. Considering the detrimental effects of SENP1 deficiency in heart diseases, we need to seriously consider cardiovascular side effects while applying systemic SENP1 blockers to suppress tumors. Accordingly, manipulating SENP1 expression requires an accurate delivery system, such as adenovirus-associated virus and nanocarrier delivery system. Furthermore, some novel anti-tumor strategies need to be further studied to manipulate SENP1 expression but prevent future cardiovascular diseases.

## ARTICLE INFORMATION

Received May 31, 2022; accepted September 29, 2022.

### Affiliations

Department of Cardiology, Renmin Hospital of Wuhan University, Wuhan, PR China (D.Y., D.F., Z.G., F.L., M.W., P.A., Z.Y., Q.T.); and Hubei Key Laboratory of Metabolic and Chronic Diseases, Wuhan, PR China (D.Y., D.F., Z.G., F.L., M.W., P.A., Z.Y., Q.T.).

### Acknowledgments

Author contributions: Dan Yang, Di Fan, and Qi-Zhu Tang contributed to the conception and design of the study; Dan Yang, Zhen Guo, Fang-Yuan Liu, Ming-Yu Wang, and Peng An conducted the experiments; Di Fan and Zhen Guo contributed to data analysis; the first draft of the manuscript was written by Dan Yang; Zheng Yang and Qi-Zhu Tang critically revised the manuscript. Qi-Zhu Tang designed all of the experiments, supervised and funded the study. All authors contributed to the article and approved the submitted version.

### Sources of Funding

This work was supported by grants from the Key Project of the National Natural Science Foundation (81530012) and National Key R&D Program of China (2018YFC1311300).

### Disclosures

None.

### Supplemental Material

Table S1  
Figures S1–S8

## REFERENCES

1. Nakamura M, Sadoshima J. Mechanisms of physiological and pathological cardiac hypertrophy. *Nat Rev Cardiol*. 2018;15:387–407. doi: [10.1038/s41569-018-0007-y](https://doi.org/10.1038/s41569-018-0007-y)

2. Truby LK, Rogers JG. Advanced heart failure: epidemiology, diagnosis, and therapeutic advances. *JACC Heart Fail.* 2020;8:523–536. doi: [10.1016/j.jchf.2020.01.014](https://doi.org/10.1016/j.jchf.2020.01.014)
3. Zhu L, Li C, Liu Q, Xu W, Zhou X. Molecular biomarkers in cardiac hypertrophy. *J Cell Mol Med.* 2019;23:1671–1677. doi: [10.1111/jcmm.14129](https://doi.org/10.1111/jcmm.14129)
4. Yildiz M, Oktay AA, Stewart MH, Milani RV, Ventura HO, Lavie CJ. Left ventricular hypertrophy and hypertension. *Prog Cardiovasc Dis.* 2020;63:10–21. doi: [10.1016/j.pcad.2019.11.009](https://doi.org/10.1016/j.pcad.2019.11.009)
5. Yang D, Liu HQ, Liu FY, Tang N, Guo Z, Ma SQ, An P, Wang MY, Wu HM, Yang Z, et al. The roles of noncardiomyocytes in cardiac remodeling. *Int J Biol Sci.* 2020;16:2414–2429. doi: [10.7150/ijbs.47180](https://doi.org/10.7150/ijbs.47180)
6. Flotho A, Melchior F. Sumoylation: a regulatory protein modification in health and disease. *Annu Rev Biochem.* 2013;82:357–385. doi: [10.1146/annurev-biochem-061909-093311](https://doi.org/10.1146/annurev-biochem-061909-093311)
7. Hotz PW, Müller S, Mandler L. SUMO-specific isopeptidases tuning cardiac SUMOylation in health and disease. *Front Mol Biosci.* 2021;8:786136. doi: [10.3389/fmolb.2021.786136](https://doi.org/10.3389/fmolb.2021.786136)
8. Kunz K, Piller T, Müller S. SUMO-specific proteases and isopeptidases of the SENP family at a glance. *J Cell Sci.* 2018;131:jcs211904. doi: [10.1242/jcs.211904](https://doi.org/10.1242/jcs.211904)
9. Taghvaei S, Sabouni F, Minuchehr Z. Evidence of omics, immune infiltration, and pharmacogenomic for SENP1 in the Pan-cancer cohort. *Front Pharmacol.* 2021;12:700454. doi: [10.3389/fphar.2021.700454](https://doi.org/10.3389/fphar.2021.700454)
10. Gu J, Fan Y, Liu X, Zhou L, Cheng J, Cai R, Xue S. SENP1 protects against myocardial ischaemia/reperfusion injury via a HIF1 $\alpha$ -dependent pathway. *Cardiovasc Res.* 2014;104:83–92. doi: [10.1093/cvr/cvu177](https://doi.org/10.1093/cvr/cvu177)
11. Cai R, Gu J, Sun H, Liu X, Mei W, Qi Y, Xue S, Ren S, Rabinowitz JE, Wang Y, et al. Induction of SENP1 in myocardium contributes to abnormalities of mitochondria and cardiomyopathy. *J Mol Cell Cardiol.* 2015;79:115–122. doi: [10.1016/j.yjmcc.2014.11.014](https://doi.org/10.1016/j.yjmcc.2014.11.014)
12. Ma ZG, Yuan YP, Zhang X, Xu SC, Kong CY, Song P, Li N, Tang QZ. C1q-tumour necrosis factor-related protein-3 exacerbates cardiac hypertrophy in mice. *Cardiovasc Res.* 2019;115:1067–1077. doi: [10.1093/cvr/cvy279](https://doi.org/10.1093/cvr/cvy279)
13. Lu X, He Y, Tang C, Wang X, Que L, Zhu G, Liu L, Ha T, Chen Q, Li C, et al. Triad3A attenuates pathological cardiac hypertrophy involving the augmentation of ubiquitination-mediated degradation of TLR4 and TLR9. *Basic Res Cardiol.* 2020;115:19. doi: [10.1007/s00395-020-0779-1](https://doi.org/10.1007/s00395-020-0779-1)
14. Wu J, Lei H, Zhang J, Chen X, Tang C, Wang W, Xu H, Xiao W, Gu W, Wu Y. Momordin Ic, a new natural SENP1 inhibitor, inhibits prostate cancer cell proliferation. *Oncotarget.* 2016;7:58995–59005. doi: [10.18632/oncotarget.10636](https://doi.org/10.18632/oncotarget.10636)
15. Fan D, Yang Z, Liu FY, Jin YG, Zhang N, Ni J, Yuan Y, Liao HH, Wu QQ, Xu M, et al. Sesamin protects against cardiac remodeling via Sirt3/ROS pathway. *Cell Physiol Biochem.* 2017;44:2212–2227. doi: [10.1159/000486026](https://doi.org/10.1159/000486026)
16. Ma SQ, Guo Z, Liu FY, Hasan SG, Yang D, Tang N, An P, Wang MY, Wu HM, Yang Z, et al. 6-gingerol protects against cardiac remodeling by inhibiting the p38 mitogen-activated protein kinase pathway. *Acta Pharmacol Sin.* 2021;42:1575–1586. doi: [10.1038/s41401-020-00587-z](https://doi.org/10.1038/s41401-020-00587-z)
17. Liu FY, Fan D, Yang Z, Tang N, Guo Z, Ma SQ, Ma ZG, Wu HM, Deng W, Tang QZ. TLR9 is essential for HMGB1-mediated post-myocardial infarction tissue repair through affecting apoptosis, cardiac healing, and angiogenesis. *Cell Death Dis.* 2019;10:480. doi: [10.1038/s41411-019-1718-7](https://doi.org/10.1038/s41411-019-1718-7)
18. Guo Z, Tuo H, Tang N, Liu FY, Ma SQ, An P, Yang D, Wang MY, Fan D, Yang Z, et al. Neuraminidase 1 deficiency attenuates cardiac dysfunction, oxidative stress, fibrosis, inflammatory via AMPK-SIRT3 pathway in diabetic cardiomyopathy mice. *Int J Biol Sci.* 2022;18:826–840. doi: [10.7150/ijbs.65938](https://doi.org/10.7150/ijbs.65938)
19. She P, Zhang H, Peng X, Sun J, Gao B, Zhou Y, Zhu X, Hu X, Lai KS, Wong J, et al. The gridlock transcriptional repressor impedes vertebrate heart regeneration by restricting expression of lysine methyltransferase. *Development.* 2020;147:dev190678. doi: [10.1242/dev.190678](https://doi.org/10.1242/dev.190678)
20. Zhang X, Patel D, Xu Q, Veenstra R. Differences in functional expression of Connexin43 and Na(V)1.5 by Pan- and class-selective histone deacetylase inhibition in heart. *Int J Mol Sci.* 2018;19:2288. doi: [10.3390/ijms19082288](https://doi.org/10.3390/ijms19082288)
21. Rohrbach S, Muller-Werdan U, Werdan K, Koch S, Gellerich NF, Holtz J. Apoptosis-modulating interaction of the neuregulin/erbB pathway with anthracyclines in regulating Bcl-xS and Bcl-xL in cardiomyocytes. *J Mol Cell Cardiol.* 2005;38:485–493. doi: [10.1016/j.yjmcc.2004.12.013](https://doi.org/10.1016/j.yjmcc.2004.12.013)
22. Fu YL, Tao L, Peng FH, Zheng NZ, Lin Q, Cai SY, Wang Q. GJA1-20k attenuates ang II-induced pathological cardiac hypertrophy by regulating gap junction formation and mitochondrial function. *Acta Pharmacol Sin.* 2021;42:536–549. doi: [10.1038/s41401-020-0459-6](https://doi.org/10.1038/s41401-020-0459-6)
23. Cheng J, Kang X, Zhang S, Yeh ET. SUMO-specific protease 1 is essential for stabilization of HIF1 $\alpha$  during hypoxia. *Cell.* 2007;131:584–595. doi: [10.1016/j.cell.2007.08.045](https://doi.org/10.1016/j.cell.2007.08.045)
24. Dong W, Zhu X, Liu X, Zhao X, Lei X, Kang L, Liu L. Role of the SENP1-SIRT1 pathway in hyperoxia-induced alveolar epithelial cell injury. *Free Radic Biol Med.* 2021;173:142–150. doi: [10.1016/j.freeradbiomed.2021.07.027](https://doi.org/10.1016/j.freeradbiomed.2021.07.027)
25. Wang T, Cao Y, Zheng Q, Tu J, Zhou W, He J, Zhong J, Chen Y, Wang J, Cai R, et al. SENP1-Sirt3 signaling controls mitochondrial protein acetylation and metabolism. *Mol Cell.* 2019;75:823–834.e825. doi: [10.1016/j.molcel.2019.06.008](https://doi.org/10.1016/j.molcel.2019.06.008)
26. He J, Shangguan X, Zhou W, Cao Y, Zheng Q, Tu J, Hu G, Liang Z, Jiang C, Deng L, et al. Glucose limitation activates AMPK coupled SENP1-Sirt3 signalling in mitochondria for T cell memory development. *Nat Commun.* 2021;12:4371. doi: [10.1038/s41467-021-24619-2](https://doi.org/10.1038/s41467-021-24619-2)
27. Bawa-Khalife T, Yang FM, Riitho J, Lin HK, Cheng J, Yeh ET. SENP1 regulates PTEN stability to dictate prostate cancer development. *Oncotarget.* 2017;8:17651–17664. doi: [10.18632/oncotarget.13283](https://doi.org/10.18632/oncotarget.13283)
28. Zheng C, Li D, Zhan W, He K, Yang H. Downregulation of SENP1 suppresses LPS-induced macrophage inflammation by elevating Sp3 SUMOylation and disturbing Sp3-NF- $\kappa$ B interaction. *Am J Transl Res.* 2020;12:7439–7448.
29. Zhao L, Cheng G, Jin R, Afzal MR, Samanta A, Xuan YT, Giris M, Elias HK, Zhu Y, Davani A, et al. Deletion of Interleukin-6 attenuates pressure overload-induced left ventricular hypertrophy and dysfunction. *Circ Res.* 2016;118:1918–1929. doi: [10.1161/circresaha.116.308688](https://doi.org/10.1161/circresaha.116.308688)
30. Ye S, Luo W, Khan ZA, Wu G, Xuan L, Shan P, Lin K, Chen T, Wang J, Hu X, et al. Celastrol attenuates angiotensin II-induced cardiac remodeling by targeting STAT3. *Circ Res.* 2020;126:1007–1023. doi: [10.1161/circresaha.119.315861](https://doi.org/10.1161/circresaha.119.315861)
31. Lu J, Xu S, Huo Y, Sun D, Hu Y, Wang J, Zhang X, Wang P, Li Z, Liang M, et al. Sorting nexin 3 induces heart failure via promoting retromer-dependent nuclear trafficking of STAT3. *Cell Death Differ.* 2021;28:2871–2887. doi: [10.1038/s41418-021-00789-w](https://doi.org/10.1038/s41418-021-00789-w)
32. Su SA, Yang D, Wu Y, Xie Y, Zhu W, Cai Z, Shen J, Fu Z, Wang Y, Jia L, et al. EphrinB2 regulates cardiac fibrosis through modulating the interaction of Stat3 and TGF- $\beta$ /Smad3 signaling. *Circ Res.* 2017;121:617–627. doi: [10.1161/circresaha.117.311045](https://doi.org/10.1161/circresaha.117.311045)
33. Johnson DE, O'Keefe RA, Grandis JR. Targeting the IL-6/JAK/STAT3 signalling axis in cancer. *Nat Rev Clin Oncol.* 2018;15:234–248. doi: [10.1038/nrclinonc.2018.8](https://doi.org/10.1038/nrclinonc.2018.8)
34. Shangguan X, He J, Ma Z, Zhang W, Ji Y, Shen K, Yue Z, Li W, Xin Z, Zheng Q, et al. SUMOylation controls the binding of hexokinase 2 to mitochondria and protects against prostate cancer tumorigenesis. *Nat Commun.* 2021;12:1812. doi: [10.1038/s41467-021-22163-7](https://doi.org/10.1038/s41467-021-22163-7)
35. Cui CP, Wong CC, Kai AK, Ho DW, Lau EY, Tsui YM, Chan LK, Cheung TT, Chok KS, Chan ACY, et al. SENP1 promotes hypoxia-induced cancer stemness by HIF-1 $\alpha$  deSUMOylation and SENP1/HIF-1 $\alpha$  positive feedback loop. *Gut.* 2017;66:2149–2159. doi: [10.1136/gutjnl-2016-313264](https://doi.org/10.1136/gutjnl-2016-313264)
36. Mandler L, Braun T, Müller S. The ubiquitin-like SUMO system and heart function: from development to disease. *Circ Res.* 2016;118:132–144. doi: [10.1161/circresaha.115.307730](https://doi.org/10.1161/circresaha.115.307730)
37. Lee A, Jeong D, Mitsuyama S, Oh JG, Liang L, Ikeda Y, Sadoshima J, Hajjar RJ, Kho C. The role of SUMO-1 in cardiac oxidative stress and hypertrophy. *Antioxid Redox Signal.* 2014;21:1986–2001. doi: [10.1089/ars.2014.5983](https://doi.org/10.1089/ars.2014.5983)
38. Oh JG, Watanabe S, Lee A, Gorski PA, Lee P, Jeong D, Liang L, Liang Y, Baccarini A, Sahoo S, et al. miR-146a suppresses SUMO1 expression and induces cardiac dysfunction in maladaptive hypertrophy. *Circ Res.* 2018;123:673–685. doi: [10.1161/circresaha.118.312751](https://doi.org/10.1161/circresaha.118.312751)
39. Gupta MK, McLendon PM, Gulick J, James J, Khalili K, Robbins J. UBC9-mediated Sumoylation favorably impacts cardiac function in compromised hearts. *Circ Res.* 2016;118:1894–1905. doi: [10.1161/circresaha.115.308268](https://doi.org/10.1161/circresaha.115.308268)
40. Harhous Z, Booz GW, Ovize M, Bidaux G, Kurdi M. An update on the multifaceted roles of STAT3 in the heart. *Front Cardiovasc Med.* 2019;6:150. doi: [10.3389/fcvm.2019.00150](https://doi.org/10.3389/fcvm.2019.00150)
41. Kunisada K, Negoro S, Tone E, Funamoto M, Osugi T, Yamada S, Okabe M, Kishimoto T, Yamauchi-Takahara K. Signal transducer and activator of transcription 3 in the heart transduces not only a hypertrophic signal but a protective signal against doxorubicin-induced cardiomyopathy. *Proc Natl Acad Sci USA.* 2000;97:315–319. doi: [10.1073/pnas.97.1.315](https://doi.org/10.1073/pnas.97.1.315)

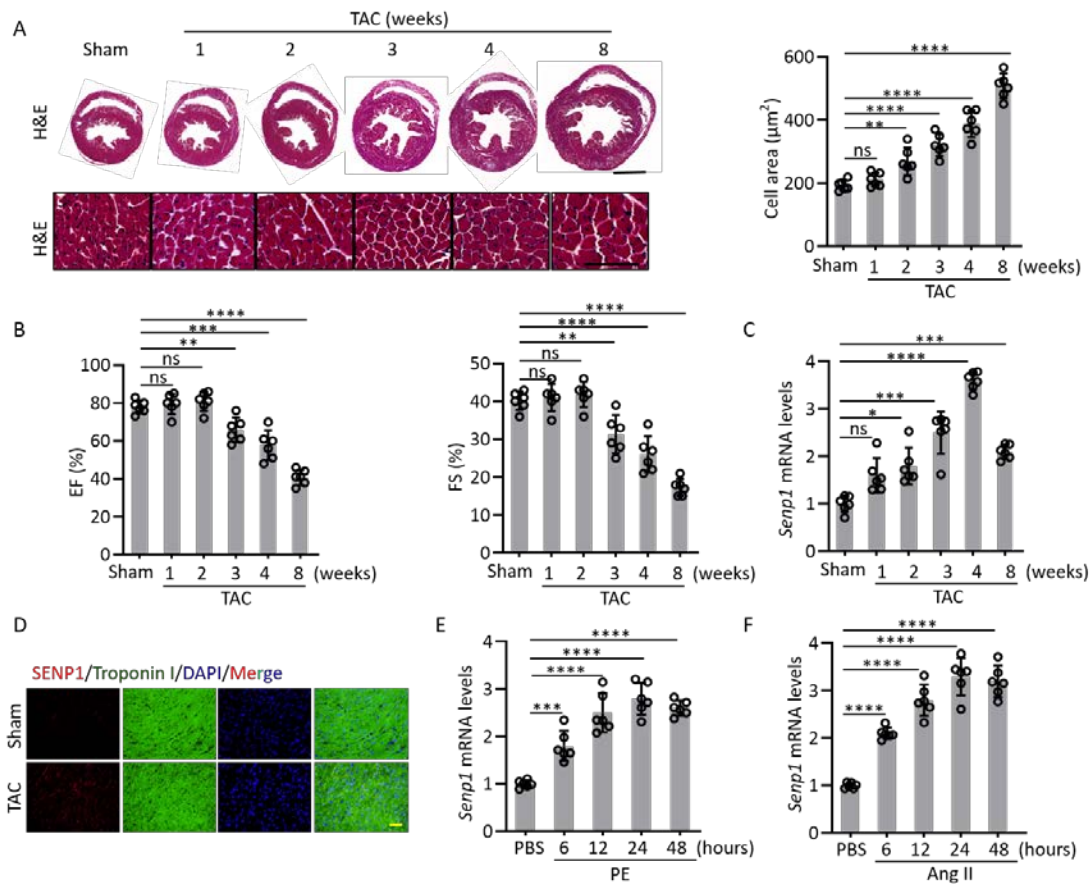
42. Mir SA, Chatterjee A, Mitra A, Pathak K, Mahata SK, Sarkar S. Inhibition of signal transducer and activator of transcription 3 (STAT3) attenuates interleukin-6 (IL-6)-induced collagen synthesis and resultant hypertrophy in rat heart. *J Biol Chem*. 2012;287:2666–2677. doi: [10.1074/jbc.M111.246173](https://doi.org/10.1074/jbc.M111.246173)
43. Uozumi H, Hiroi Y, Zou Y, Takimoto E, Toko H, Niu P, Shimoyama M, Yazaki Y, Nagai R, Komuro I. gp130 plays a critical role in pressure overload-induced cardiac hypertrophy. *J Biol Chem*. 2001;276:23115–23119. doi: [10.1074/jbc.M100814200](https://doi.org/10.1074/jbc.M100814200)
44. Verma SK, Krishnamurthy P, Barefield D, Singh N, Gupta R, Lambers E, Thal M, Mackie A, Hoxha E, Ramirez V, et al. Interleukin-10 treatment attenuates pressure overload-induced hypertrophic remodeling and improves heart function via signal transducers and activators of transcription 3-dependent inhibition of nuclear factor- $\kappa$ B. *Circulation*. 2012;126:418–429. doi: [10.1161/circulationaha.112.112185](https://doi.org/10.1161/circulationaha.112.112185)
45. Johnson AW, Kinzenbaw DA, Modrick ML, Faraci FM. Small-molecule inhibitors of signal transducer and activator of transcription 3 protect against angiotensin II-induced vascular dysfunction and hypertension. *Hypertension (Dallas, Tex: 1979)*. 2013;61:437–442. doi: [10.1161/hypertensionaha.111.00299](https://doi.org/10.1161/hypertensionaha.111.00299)
46. Lin H, Smith N, Spigelman AF, Suzuki K, Ferdaoussi M, Alghamdi TA, Lewandowski SL, Jin Y, Bautista A, Wang YW, et al.  $\beta$ -Cell knockout of SENP1 reduces responses to incretins and worsens oral glucose tolerance in high-fat diet-fed mice. *Diabetes*. 2021;70:2626–2638. doi: [10.2337/db20-1235](https://doi.org/10.2337/db20-1235)
47. Tham YK, Bernardo BC, Ooi JY, Weeks KL, McMullen JR. Pathophysiology of cardiac hypertrophy and heart failure: signaling pathways and novel therapeutic targets. *Arch Toxicol*. 2015;89:1401–1438. doi: [10.1007/s00204-015-1477-x](https://doi.org/10.1007/s00204-015-1477-x)
48. Shimizu I, Minamino T. Physiological and pathological cardiac hypertrophy. *J Mol Cell Cardiol*. 2016;97:245–262. doi: [10.1016/j.yjmcc.2016.06.001](https://doi.org/10.1016/j.yjmcc.2016.06.001)
49. Li Q, Li C, Elnwasany A, Sharma G, An YA, Zhang G, Elhelaly WM, Lin J, Gong Y, Chen G, et al. PKM1 exerts critical roles in cardiac remodeling under pressure overload in the heart. *Circulation*. 2021;144:712–727. doi: [10.1161/circulationaha.121.054885](https://doi.org/10.1161/circulationaha.121.054885)
50. Tang X, Pan L, Zhao S, Dai F, Chao M, Jiang H, Li X, Lin Z, Huang Z, Meng G, et al. SNO-MLP (S-Nitrosylation of muscle LIM protein) facilitates myocardial hypertrophy through TLR3 (toll-like receptor 3)-mediated RIP3 (receptor-interacting protein kinase 3) and NLRP3 (NOD-like receptor pyrin domain containing 3) inflammasome activation. *Circulation*. 2020;141:984–1000. doi: [10.1161/circulationaha.119.042336](https://doi.org/10.1161/circulationaha.119.042336)
51. Wei J, Wang H, Zheng Q, Zhang J, Chen Z, Wang J, Ouyang L, Wang Y. Recent research and development of inhibitors targeting sentrin-specific protease 1 for the treatment of cancers. *Eur J Med Chem*. 2022;241:114650. doi: [10.1016/j.ejmech.2022.114650](https://doi.org/10.1016/j.ejmech.2022.114650)

## **SUPPLEMENTAL MATERIAL**

**Table S1. Primer sequences used in the qRT-PCR experiments**

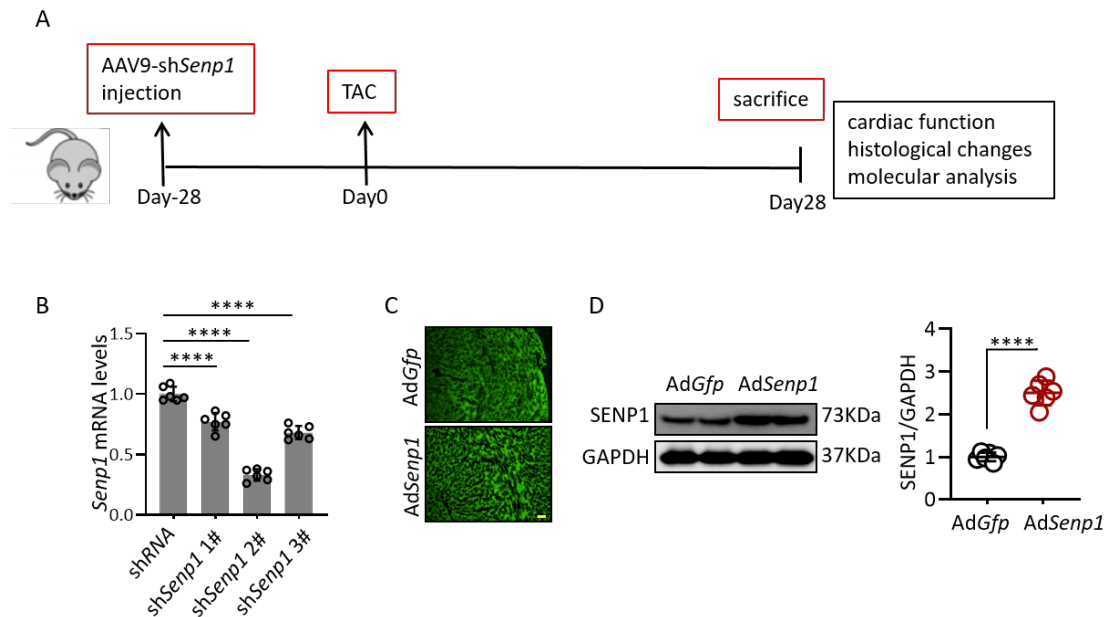
Genes	Forward (5'-3')	Reverse (5'-3')
Mouse GAPDH	ACTCCACTCACGGCAAATTC	TCTCCATGGTGGTGAAGACA
Mouse SENP1	CAGCAGATGAATGGAAGTGA	CCGGAAGTATGGCATGTGT
Mouse ANP	ACCTGCTAGACCACCTGGAG	CCTTGGCTGTTATCTTCGGTACCGG
Mouse BNP	GTCAGTCGTTTGGGCTGTAAC	AGACCCAGGCAGAGTCAGAA
Mouse $\beta$ -MHC	CCGAGTCCCAGGTCAACAA	CTTACGGGCACCCTTGGA
Mouse $\alpha$ -MHC	GTCCAAGTTCCGCAAGGT	AGGGTCTGCTGGAGAGGTTA
Mouse Col1	CCCAACCCAGAGATCCCATT	GAAGCACAGGAGCAGGTGTAGA
Mouse Col3	TCCCCTGGAATCTGTGAATC	TGAGTCGAATTGGGGAGAAT
Rat GAPDH	GACATGCCGCCTGGAGAAAC	AGCCCAGGATGCCCTTTAGT
Rat SENP1	CTCAGGCTTCCAGAGGACC	ACTGCTTGTAGAACCCGTGA
Rat ANP	AAAGCAAACCTGAGGGCTCTGCTCG	TTCGGTACCGGAAGCTGTTGCA
Rat $\beta$ -MHC	TCTGGACAGCTCCCCATTCT	CAAGGCTAACCTGGAGAAGATG

**Figure S1. Hypertrophic stimulation leads to the upregulation of SENP1 *in vivo* and *in vitro*.**



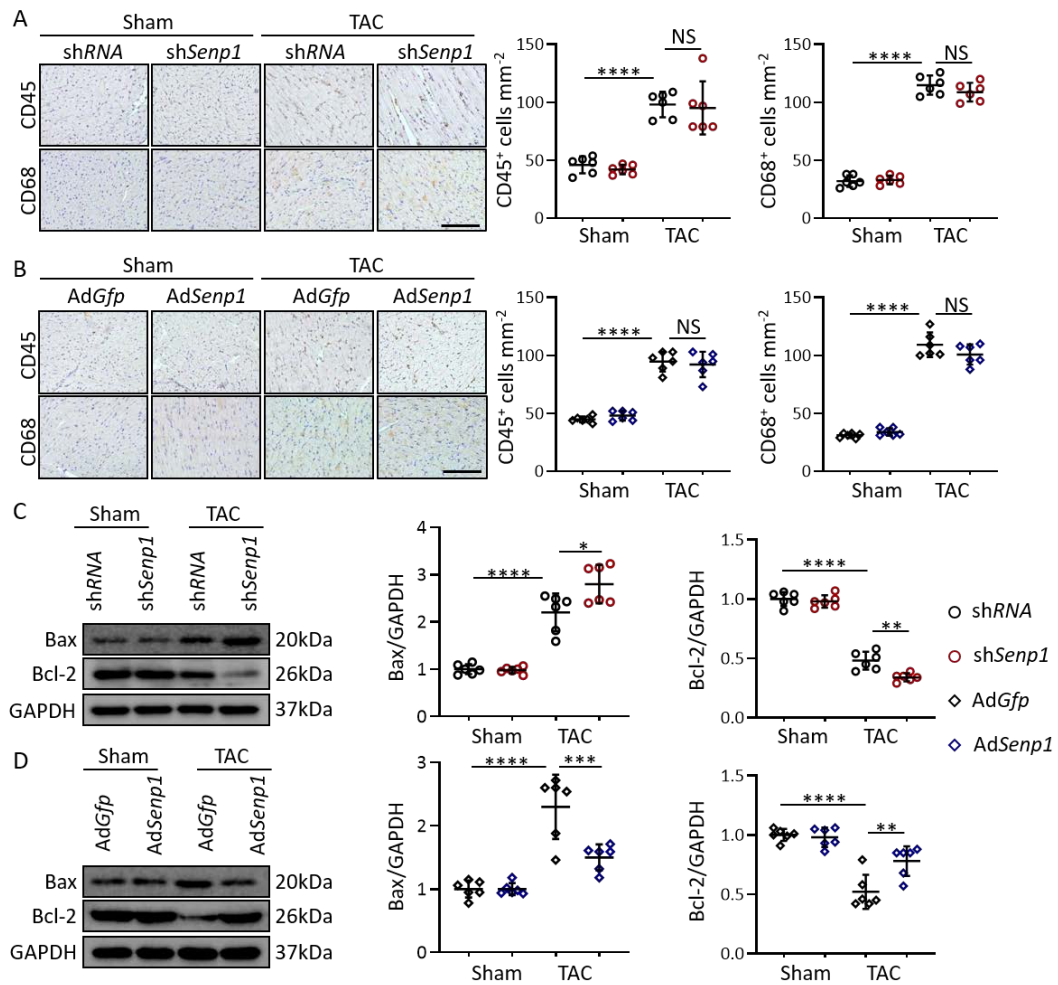
(A) Histological analyses of the H&E staining and quantification of the average cross-sectional areas in WT mice at 1, 2, 3, 4, and 8 wk after TAC surgery (n=6 per group). Scale bar, 2mm (top), 100µm (bottom). (B) Echocardiographic assessments of EF% and FS% in mice in the indicated groups (n=6 per group). (C) qPCR analysis for SENP1 expression in mice subjected to sham or TAC operations in the indicated times (n=6 per group). mRNA expression was quantified and normalized to GAPDH. (D) Representative images for immunofluorescence staining of cardiac Troponin I (green) and SENP1 (red) in WT mouse hearts with sham or TAC operation for 4 weeks. Scale bar, 50µm. (E) qPCR analysis for SENP1 expression in NRCMs treated with PE (50 µM) in the indicated times (n=6 independent experiments). mRNA expression was quantified and normalized to GAPDH. (F) qPCR analysis for SENP1 expression in NRCMs treated with Ang II (1 µM) in the indicated times (n=6 independent experiments). mRNA expression was quantified and normalized to GAPDH. Values represent the mean ± SD. Significance was calculated using 1-way ANOVA with Bonferroni's post-hoc test (A, B, E and F) and Kruskal-Wallis (C). \*, P <0.05; \*\*, P <0.01; \*\*\*, P <0.001; \*\*\*\*, P < 0.0001; NS, not significant. SENP1, Sentrin/SUMO-specific protease 1; TAC, transverse aortic constriction; NRCMs, neonatal rat cardiomyocytes; PE, phenylephrine; Ang II, Angiotensin II.

**Figure S2. The efficiency of AAV9-mediated SENP1 knockdown and adenovirus-mediated SENP1 overexpression.**



(A) Schema of the procedure for injection of AAV9 carrying *shSenp1*. (B) The inhibitory efficiency of three constructed AAV9 carrying *shSenp1*, among which the second had the highest inhibitory efficiency. (C) Fluorescence intensity of cardiac sections was detected by fluorescence microscope 2 weeks after intramyocardial injection. Scale bar, 100 $\mu$ m. (D) Representative western blot analysis and quantitative data for SENP1 protein levels in mouse hearts transduced with *AdGfp* or *AdSenp1* (n=6 per group). Protein expression was quantified and normalized to GAPDH. Values represent the mean  $\pm$  SD. Data were analyzed by 1-way ANOVA with Bonferroni's post-hoc test (B) and unpaired Student's t-test (D). \*, P < 0.05; \*\*, P < 0.01; \*\*\*, P < 0.001; \*\*\*\*, P < 0.0001. SENP1, Sentrin/SUMO-specific protease 1; TAC, transverse aortic constriction; GFP, green fluorescence protein.

**Figure S3. The effects of SENP1 on cardiac inflammation and apoptosis induced by pressure overload.**

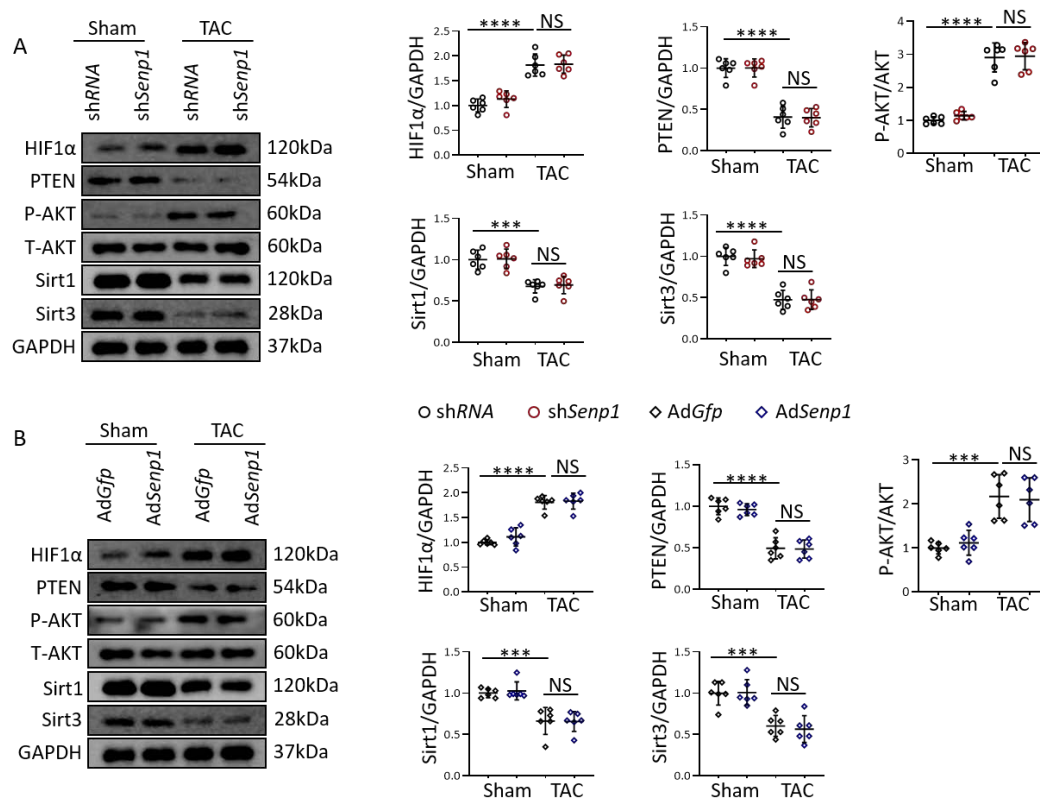


**(A)** Immunohistochemistry staining and quantitative data for CD45 and CD68 in cardiac cross-sections from shRNA or shSenp1 treated mice following 4 weeks of sham or TAC operations (n=6 per group). Scale bar, 100  $\mu$ m. **(B)** Immunohistochemistry staining and quantitative data for CD45 and CD68 in cardiac cross-sections from AdGfp or AdSenp1 treated mice following 4 weeks of sham or TAC operations (n=6 per group). Scale bar, 100  $\mu$ m. **(C)** Representative western blot analysis and quantitative data for Bax and Bcl-2 protein levels in shRNA or shSenp1 treated mice following 4 weeks of sham or TAC operations (n=6 per group). Protein expression was quantified and normalized to GAPDH. **(D)** Representative western blot analysis and quantitative data for Bax and Bcl-2 protein levels in AdGfp or AdSenp1 treated mice following 4 weeks of sham or TAC operations (n=6 per group). Protein expression was quantified and normalized to GAPDH. Values represent the mean  $\pm$  SD. All data were analyzed by 2-way ANOVA with Bonferroni's post-hoc test. \*, P < 0.05; \*\*, P < 0.01; \*\*\*, P < 0.001; \*\*\*\*, P < 0.0001; NS: not significant. SENP1, Sentrin/SUMO-specific protease 1; TAC, transverse aortic constriction; CD45,



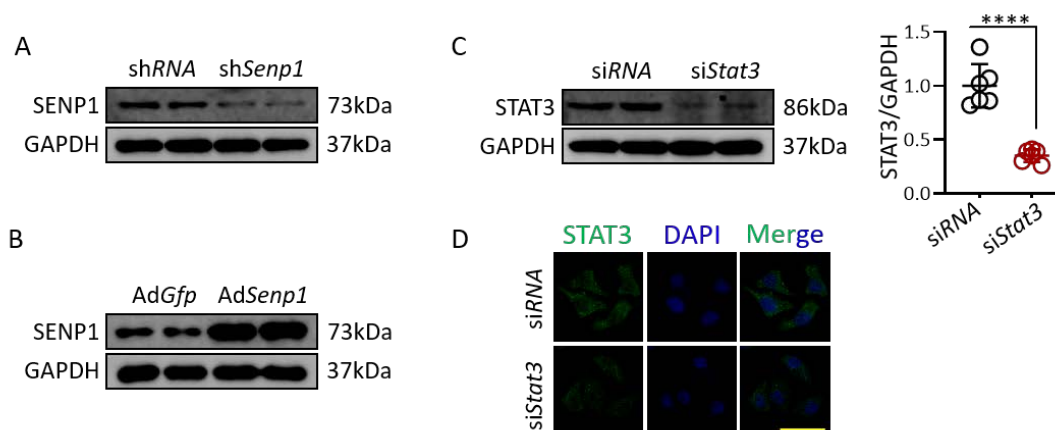
cluster of differentiation 45; CD68, cluster of differentiation 68; Bcl-2, B-cell lymphoma-2; Bax, Bcl-2-Associated X Protein.

**Figure S4. HIF1 $\alpha$ , PTEN/AKT, Sirt1, and Sirt3 signaling pathways are not involved in SENP1-regulated cardiac hypertrophy.**



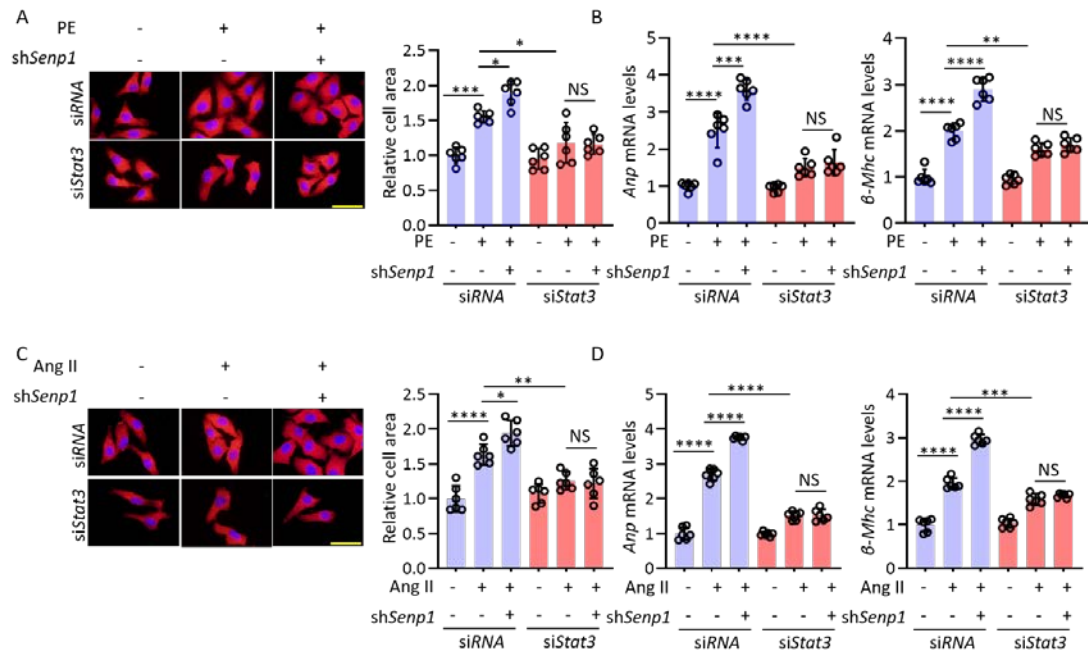
**(A)** Representative western blot analysis and quantitative data for HIF1 $\alpha$ , PTEN, P-AKT, AKT, Sirt1, and Sirt3 protein levels in cardiac extracts from shRNA and shSenp1 mice 4 weeks after TAC or sham operations (n=6 per group). Protein expression was quantified and normalized to GAPDH. **(B)** Representative western blot analysis and quantitative data for HIF1 $\alpha$ , PTEN, P-AKT, AKT, Sirt1, and Sirt3 protein levels in cardiac extracts from AdGfp and AdSenp1 mice 4 weeks after TAC or sham operations (n=6 per group). Protein expression was quantified and normalized to GAPDH. Values represent the mean  $\pm$  SD. All data were analyzed by 2-way ANOVA with Bonferroni's post-hoc test. \*, P < 0.05; \*\*, P < 0.01; \*\*\*, P < 0.001; \*\*\*\*, P < 0.0001; NS: not significant. SENP1, Sentrin/SUMO-specific protease 1; TAC, transverse aortic constriction; HIF1 $\alpha$ , hypoxia inducible factor 1-alpha; PTEN, phosphatase and tensin homolog; Sirt1, sirtuin 1; Sirt3, sirtuin 3; AKT, protein kinase B.

**Figure S5. The efficiency of gene overexpression or knockdown in cultured cells.**



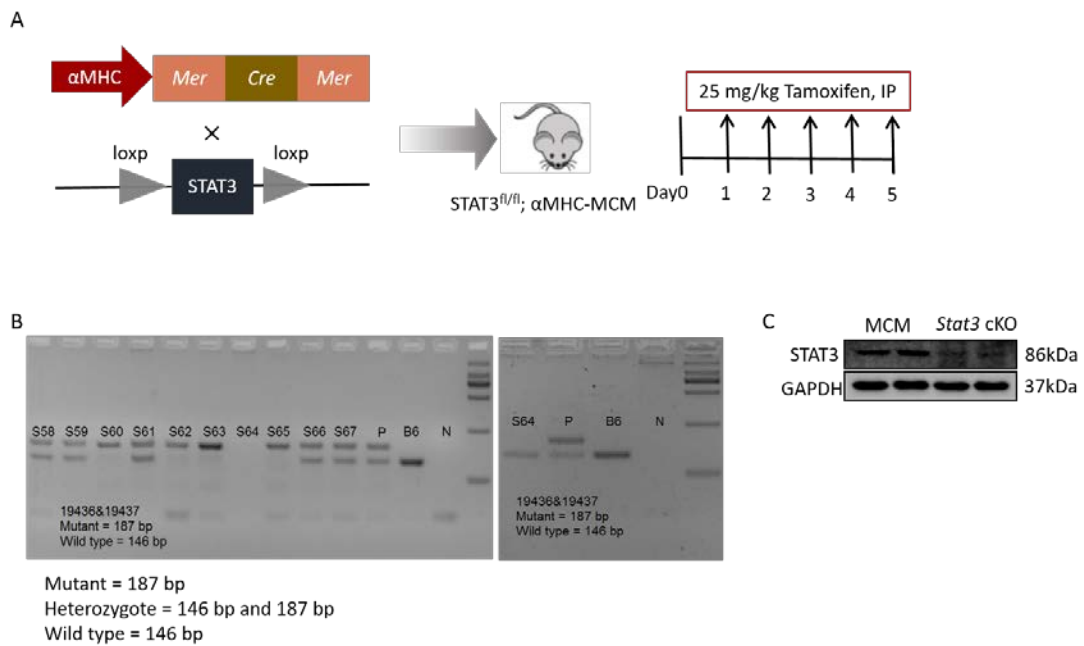
(A) Representative western blot analysis of SENP1 protein levels in shRNA and sh*Senp1* treated NRCMs. Protein expression was normalized to GAPDH. (B) Representative western immunoblots for SENP1 protein levels in Ad*Gfp* and Ad*Senp1* treated NRCMs. Protein expression was normalized to GAPDH. (C) Representative western blot analysis and quantitative data for STAT3 protein levels in siRNA or si*Stat3* treated NRCMs (n=6 independent experiments). Protein expression was quantified and normalized to GAPDH. (D) Representative images for immunofluorescence staining of STAT3 in siRNA or si*Stat3* treated H9c2 cells. Scale bar, 50µm. Values represent the mean  $\pm$  SD. Unpaired Student's t-test. \*, P < 0.05; \*\*, P < 0.01; \*\*\*, P < 0.001; \*\*\*\*, P < 0.0001. SENP1, Sentrin/SUMO-specific protease 1; STAT3, signal transducer and activator of transcription 3.

**Figure S6. Inhibition of STAT3 negates the detrimental effects of SENP1 deficiency on hypertrophic response in cultured H9c2 cells.**



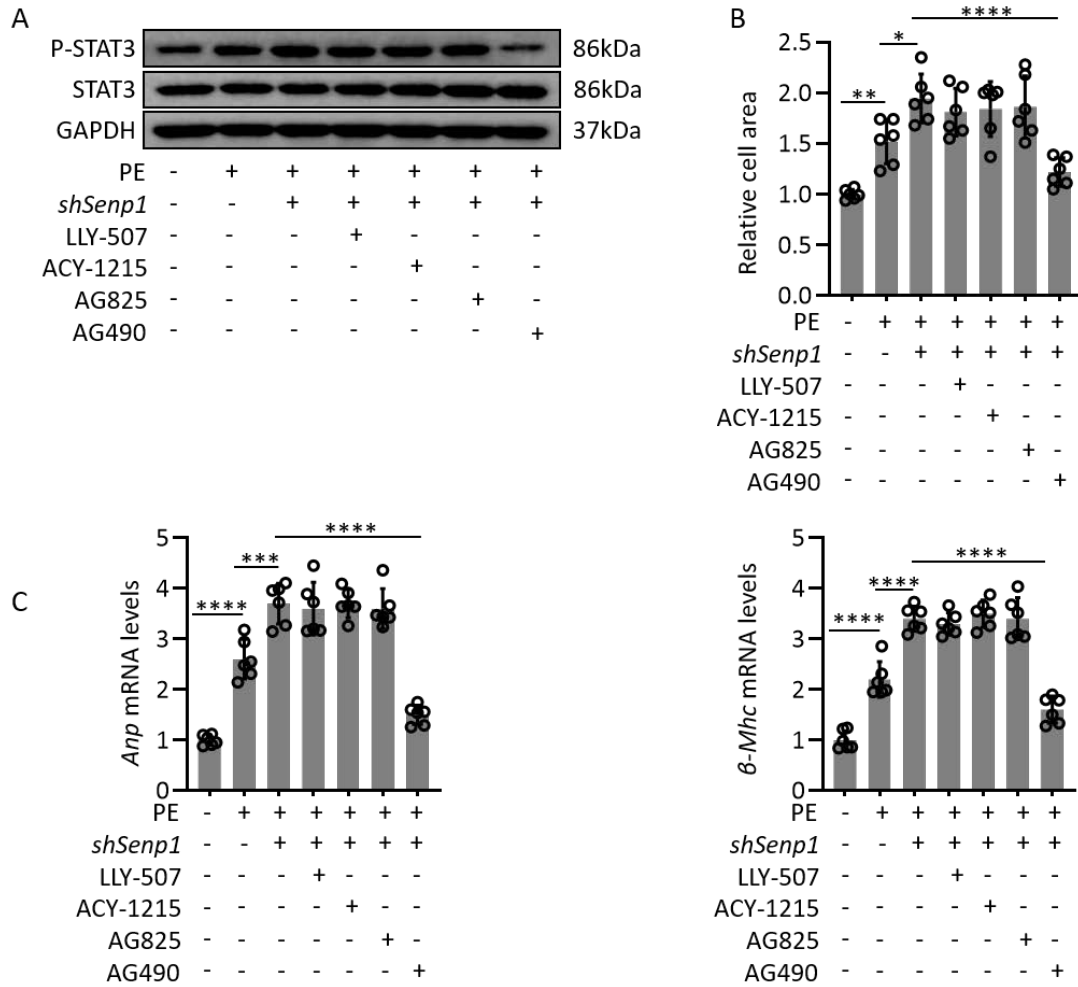
(A) Representative images and quantitative data for immunofluorescence staining of  $\alpha$ -actinin in H9c2 cells in the indicated groups (n=6 independent experiments). Scale bar, 50 $\mu$ m. (B) qPCR analysis for hypertrophic gene expression in H9c2 cells in the indicated groups (n=6 independent experiments). mRNA expression was quantified and normalized to GAPDH. (C) Representative images and quantitative data for immunofluorescence staining of  $\alpha$ -actinin in H9c2 cells in the indicated groups (n=6 independent experiments). Scale bar, 50 $\mu$ m. (D) qPCR analysis for hypertrophic gene expression in H9c2 cells in the indicated groups (n=6 independent experiments). mRNA expression was quantified and normalized to GAPDH. Values represent the mean  $\pm$  SD. All data were analyzed by 2-way ANOVA with Bonferroni's post-hoc test. \*, P < 0.05; \*\*, P < 0.01; \*\*\*, P < 0.001; \*\*\*\*, P < 0.0001; NS: not significant. SENP1, Sentrin/SUMO-specific protease 1; STAT3, signal transducer and activator of transcription 3; PE, phenylephrine; Ang II, Angiotensin II; ANP, atrial natriuretic peptide;  $\beta$ -MHC,  $\beta$ -myosin heavy chain.

**Figure S7. The generation of cardiomyocyte-specific STAT3 knockout mice.**



**(A)** Schematic of the generation of STAT3 conditional knockout mice. **(B)** The genotypic identification of *Stat3* cKO mice. The WT allele was shown to 146 bp, the mutant allele 187bp, and the heterozygote allele generated 146 and 187bp bands. **(C)** Representative western blots for STAT3 protein levels in  $\alpha$ MHC-MCM and *Stat3* cKO mice. STAT3, signal transducer and activator of transcription 3.

**Figure S8. JAK2 inhibitor negates the detrimental effects of SENP1 deficiency on hypertrophic response in cultured NRCMs.**



(A) Representative western blot analysis of P-STAT3 and STAT3 protein levels in NRCMs treated by *shSenp1*, PE, plus Smyd2 inhibitor LLY-507, HDAC6 inhibitor ACY-1215, ErbB2 inhibitor AG825, or JAK2 inhibitor AG490 (n=6 independent experiments). Protein expression was quantified and normalized to GAPDH. (B) Quantitative data for cell areas of NRCMs in the indicated groups (n=6 independent experiments). (C) qPCR analysis for hypertrophic gene expression in NRCMs in the indicated groups (n=6 independent experiments). mRNA expression was quantified and normalized to GAPDH. Values represent the mean  $\pm$  SD. All data were analyzed by 1-way ANOVA with Bonferroni's post-hoc test. \*, P < 0.05; \*\*, P < 0.01; \*\*\*, P < 0.001; \*\*\*\*, P < 0.0001. SENP1, Sentrin/SUMO-specific protease 1; STAT3, signal transducer and activator of transcription 3; PE, phenylephrine; ANP, atrial natriuretic peptide;  $\beta$ -MHC,  $\beta$ -myosin heavy chain.